Journal of Earth and Atmospheric Research

THE IMPACT OF MAGNETOTELLURIC BASED NATURAL ELECTRIC FIELD TECHNIQUE IN EARTH'S CONDUCTIVITY ASSESSMENT OF A CASSAVA PROCESSING SITE SOUTH-WEST NIGERIA

Ishola, S. A.

Department of Earth Sciences, Olabisi Onabanjo University
Ago-Iwoye, Ogun State, Nigeria.

Article History
Received: 03-12-2024
Accepted: 15-05-2025

Keywords:
Cassava mill effluent, natural electric field, aquiferous medium, convergence, Signals, profile map

ABSTRACT

This study investigates leachate infiltration and its potential impact on groundwater system at Apete Cassava Processing Site using Natural Electric Field (NEF) technique. Five (5) different profiles of NEF measurements were carried out with NEFT5 acting as the control profile spaced at a distance of 500m away from the investigated site with the aid of PQWT-TC150 model of a typical water detector integrating the principle of nuclear magnetic resonance, magneto-telluric and induced polarization methods utilized for the NEF measurement imaging the subsurface to the depth of 150m. The data points ranged from 5 at NEFT3 to 16 at NEFT4 at a lateral distance of 15m to 80m respectively. The acquired datasets from the NEF technique were inputted into MATLAB mathematical software to generate the frequency curve and subsequent profile maps of electric potential difference. The output from NEF revealed frequency curves and subsurface images with respect to depth and profile distance. The points of convergence signals on the frequency model correspond to subsurface porous media characterized with low potential difference signatures on the profile map. The extent of the invaded zones ranged 0.08 to 0.21 mV from the top soil down to the depths of 30m to 40m respectively. The lowest and highest peak potential response of 0.8mV and 40.1mV were respectively encountered in profile NEFT4 and profile NEFT3 respectively with the delineation of zones depending on the degree of leachate invasion; NEFT1 to NEFT4 were found to be dominated with leachates from the surface to significant depths with varying contour signature of the 2D geo-section on the profile maps. These conductive media showing high points of convergence signals on the frequency model were seen as being saturated with leachates especially at the topsoil through the high conductive routes migrating along fractures as detected from the surface approaching the water table through gravity flow. Therefore, the groundwater quality may be at risk of contamination of cassava mill effluents due to the continuous infiltration of leachates from the surface invasion.

Correspondence: ishola.sakirudeen@oouagoiwoye.edu.ng

1. INTRODUCTION

Several communities in Nigeria and larger part of West Africa are well noted for processing of cassava tuber which served as the fourth largest stable food in Nigerian communities with several cassava processing mills randomly sited. Due to

lethal cyanogenic glucosides that are virulent and deleterious to the human health and overall environment, cassava tubers require processing before consumption (Padmaja, 1995). Since the processing of cassava tubers usually involves cutting, washing, soaking, grinding and fermentation, large volumes of Cassava Mill Effluents (CMEs) are generated alongside the aforementioned cassava processing activities (Izah et al., 2017; Itoba-Tombo et al., 2017). The cumulative gathering of these CMEs must be adequately monitored and consequently managed to avoid the creation of severe threats to the environment. Leachates from CMEs are inorganic chemical constituents comparable to those from landfills; they contain highly toxic materials that are released indiscriminately in their natural, untreated form into the immediate environment, thereby contaminating the subsurface and may end up polluting the surrounding groundwater indirectly through infiltration if left unchecked. Most groundwater system in Apete come from mostly shallow unconfined aquifers harnessed through hand-dug wells. CME Pollutants from these randomly sited cassava mills most often migrate their ways from the surface and gradually infiltrate the vadose zone and substantially pollute the groundwater beneath with unprecedented impacts. MacDonald et al., (2012) reported that leachates are the worst-known source of shallow groundwater contamination due to its high concentration of pollutants and its ability to easily infiltrate and contaminate the soil and groundwater thereby making these pollutants including heavy metals, organic compounds and pathogens pose significant risks to both human and environmental health. Several studies from published literatures have revealed the presence of leachate in groundwater within the vicinity of disposal sites in the Nigeria. Obueh and Odesiri (2016) noted that incessant disposal of CMEs into the soil alters the microbiological, physicochemical and mineralogical compositions of the soil environment surrounding the mills. The CMEs have the potentials of also migrating to other locations at distances relative to the disposal sites depending on the hydraulic conductivity of the subsurface geologic material. Cyanogen especially hydrogen cyanide and mycotoxins emanating from CMEs distort the soil's characteristics and structure by altering its physical, chemical and biological properties ultimately reducing its fertility and functionality. These toxins present in the effluent can lead to changes in soil pH, nutrient availability and microbial activity impacting aggregate formation and soil health with seepage into groundwater systems being of paramount concern, through leaching and cross-contamination leading to reduced crop yields, environmental degradation and negatively impacting terrestrial, aquatic life and overall water quality, thus culminating into prolonged cumulative human and animal exposure.

Leachates generally diminish the resistivity of the strata that inhabits them (Aweto, 2023) making electrical resistivity technique a suitable non-invasive method for subsurface delineation of contaminant plumes from an identifiable point source. This study intends to investigate the impact of CMEs on the soil/subsoil and the groundwater utilizing magnetotelluric technique of geophysical methods. Though, other known geophysical techniques namely gravity, seismic, electrical resistivity method among others are

essentials, natural electric field serves as a necessary preliminary tool for an excellent environmental impact assessment choice for subsurface investigation due to its principal benefits like its qualities of non-invasiveness, non-destructiveness, and capacity of proffering continuous subsurface information for a profile in areas such as groundwater probing, delineating subsurface components, evaluation of topsoil hydrological characteristics (Mor and Ravindra, 2016; Oyeyemi et al., 2020; Suleiman et al., 2023). Osinowo et al., 2020 reported that information on crucial profiling and investigations regarding leachate contamination resulting from urban and domestic dumpsites are provided by geophysical method. As a result, it is often imperative to investigate the subsurface geological information for groundwater quantity and quality based on the geophysical information carried specifically in an environment characterized with leachates. This technique has been effective in delineating, mapping and monitoring its potential migratory pattern in the soil (El-Maiguri et al., 2016). In this regards, level and degree of groundwater contamination becomes relevant as (WHO, 2000) reported that virulent and debilitating clinic conditions like typhoid, diarrhea, dysentery, cholera, and skin cancer occur widely across the globe causing over 4 % and 5 % respectively of all recorded death cases and health loss to disability. Cassava mill effluents can negatively impact human health due to the presence of cyanide and other pollutants, potentially leading to varying health problems like nausea, difficulty in breathing and headaches. Untreated effluents can contaminate water sources, impacting the quality of drinking water and potentially transmitting pathogens. Additionally, the effluents can alter soil properties, affecting crops which could be harmful when consumed by humans. Cassava processes releases cyanide (CN^-) and hydrocyanic acid (HCN) into the wastewater due to the presence of cyanogenic glycosides particularly linamarin in the plant tissues, during cassava processing steps like washing, peeling, grating, and extraction, these glycosides can be released and in turn converted to hydrogen cyanide (HCN) via enzymatic reactions (Ugwu and Agunwamba, 2021). While low levels are considered safe, exposure to higher concentrations can cause health problems; untreated cassava effluent can contaminate well water and other water sources. This can lead to the transmission of pathogens and negatively impact water quality making it unsuitable for drinking; it can cause soil degradation by altering the physicochemical properties of soil including changes in pH, nutrient levels, and microbial activity. Crops grown on contaminated soil may absorb nutrients in excess or deficit leading to potential health issues when consumed by humans. CME can induce to toxicological effects on the environments and its biota including humans, fisheries, flora and fauna. The impacts are mostly associated with physicochemical (odour, cyanide, acidic, dissolved oxygen, biological and chemical oxygen demand, conductivity) and heavy metals characteristics. Natural Electric Field (NEF) methods offer advantages over other geophysical techniques in delineating leachates by measuring the electrical potential difference in the subsurface which is affected by the presence of conductive materials like leachate thereby utilizing the principle of conductivity contrast, potential difference

measurement, anomaly detection and plume mapping coupled with their simplicity, ease of operation, and ability to provide detailed spatial coverage through frequency selection, integration with other geophysical methods like VES, hydrogeological modeling, cost- effectiveness as well as non-invasiveness (Sun, 2002; Theophilus et al., 2023; Okanigbuan, et al., 2025). They have been harnessed over the years by researchers to delineate leachate groundwater interaction with dumpsites, map leachate plumes in agricultural processing waste dumpsites and assess aquifer vulnerability around dumpsites (Akiang et al., 2022). NEF detectors are easier to handle and operate, allowing for complete and dense space coverage, deeper investigation depths, and easier interpretation compared to methods like Vertical Electric Sounding (VES). While NEF can be validated against other methods like VES, Its primary strength lies in its ease of use and ability to provide a comprehensive view of subsurface conditions, particularly in identifying leachate-contaminated zones. Other geophysical methods possess inherent limitation; VES can provide valuable information about subsurface layers, it may not be as effective at delineating leachate plumes as NEF due to its reliance on artificial electrical sources and the potential for complexities in data interpretation; dipole-dipole surveys can provide 2D images of subsurface resistivity but they require more complex equipment and interpretation and may not be as effective as NEF in delineating plumes at depth; why Electrical Resistivity Tomography Method (ERTM) can be used to map subsurface resistivity, but it may be less effective than NEF in delineating leachate plumes due to its reliance on artificially generated electrical currents and the potential for complexities in data interpretation. Therefore, while other geophysical methods can provide valuable information, NEF methods offer significant advantages in delineating leachates due to their simplicity and ease of interpretation; they are relatively simple to implement compared to other geophysical techniques requiring minimal equipment and training; dense spatial coverage; NEF detector can provide dense spatial coverage, allowing for a more comprehensive understanding of the subsurface, which is crucial for accurately mapping leachate plumes; NEF methods can provide deeper investigation depths compared to some other techniques, enabling a better understanding of the extent of leachate contamination at various subsurface levels; the data collected by NEF methods are generally easier to interprete compared to other geophysical techniques, making it simpler to identify leachate contaminated zones. NEF methods are generally more cost effective compared to other techniques making them a suitable choice for large-scale leachate mapping projects. Also, NEF can be effectively combined with other methods such as VES and dipole-dipole surveys to improve accuracy and provide a more comprehensive understanding of leachate contamination These advantages make NEF a cost-effective and efficient tool for monitoring and mapping leachate plumes, especially in areas where data collection and interpretation need to be straightforward (Ahmed and Ali, 2004). Therefore, the presence of cassava leachates in the study area is highly significant in groundwater and environmental studies.

Apete Township in Ido local Government area of Oyo state in Nigeria has rapidly increased in

population over the years due to its relative closeness to The Polytechnic; Ibadan in the state capital being the only state owned and managed tertiary institution. This increment was due to very large number of recently admitted students in the institution. Idi-oro community; a suburb of Apete, in the neighbourhood of this institution equally witnessed large influx of students and staffs from this citadel of learning and technological innovation securing accommodation in areas closer to this institution with evidence on the available hall of residences been occupied beyond their normal capacity inadvertently leading to increased demand for quality water in that vicinity. Safe water is a fundamental necessity for sustaining life and wellness. Groundwater tapped from subsurface like boreholes, hand-dug wells, and springs may not be considerably treated before becoming potable as a result of natural filtration process it must have undergone through the soil horizons and different compartment within the subsurface of the earth (Adeniji et al., 2024). The tendency of utilizing groundwater as a source of water supply for public application is highly significant. This investigation was initiated as a result of the increasing need for quality and readily available groundwater with a view to coping with the ever increasing demands for water resulting from the increased population experience coupled with the need to assess the impacts of cassava processing activities on the subsurface geological structure that can possibly invade the sanitary qualities of the groundwater system in the study area. Therefore, in this study, the magnetotelluric (natural electric field) technique of geophysical investigation was adopted utilizing the PQWT-TC150 equipment for such investigation of subsurface environment due to the conductive tendency of most contaminants, with the primary aim of monitoring and evaluating the degree of probable leachate infiltrations impacting the groundwater quality of the study area.

2.0 STUDY AREA

2.1 Location and Accessibility of Apete

The research site is located in a suburb of Apete Township in Ido local Government area of Oyo state, Nigeria. It is positioned approximately 0.73 kilometers west of Apete Motor Garage and about 1.7 kilometers south of Polytechnic Ibadan. The study area is bounded and restricted by latitude 7.4507 to 7.4518 north of the equator and longitude 3.8695 to 3.8707 east of the Greenwich Meridian. Major roads and footpaths facilitate access to this area. Figure 1 is a field photograph showing the cassava processing activities in the study area; Figure 2 is a satellite map of the study area showing the profile lines, Figure 3 is the geology map of the study area (Egbinola and Amanambu, 2014) and Figure 4 is the data acquisition map of the study area (Dare and Fatoba, 2014).

2.2 Climate and Geology

The climate of the study area is characterized by a tropical wet and dry climate (Köppen climate classification Aw, 2017); with a lengthy wet season and relatively constant temperatures throughout the year. The wet season runs from March through October, though August sees somewhat of a lull in precipitation. This lull divides the wet season into two different wet seasons. November to February forms the area's dry season, during which the typical West African harmattan occurs. The mean total rainfall of the

area is approximately 1,230 millimeters or 48 inches, falling over about 123 days. There are two peaks for rainfall, June and September (Egbinola and Amanambu, 2014). The mean daily temperature is 26.46 °C or 79.63 °F, the mean minimum is 21.42 °C or 70.56 °F, and the relative humidity is 74.55% (Amanambu, 2015).The area is naturally drained by four rivers with many tributaries: the Ona River in the North and West; the Ogbere River towards the East; the Ogunpa River flowing through the area and the Kudeti River in the Central part of the metropolis. Ogunpa River is a third-order stream with a channel length of 12.76 km and a catchment area of 54.92 km^2. Lake Eleyele is located in the northwestern part of the area, while the Osun River and the Asejire Lake border the area to the east. The vegetation pattern of the study area is a patchwork of broken forest, savannah woodland, dense thickets, and large tracts of forbs vegetation dominated by Chromolaena (Eupatorium) and Odorata (Siam weed) (Odjugo, 2009). The study area is underlain by three lithological units of the crystalline basement complex, comprising: Migmatite-Gneiss Complex (quartzite, gneissic rocks); Low to medium grade metasediments (Green schists facies, namely quartz schist and mica schist) and the Pan African Granitoids (older granites) which are syn to late tectonic intrusions (Figure 4). Topographically, the area is gentle, with surface elevation ranging from 197 m to 220 m above sea level. The study site is underlain by a basement complex, characterised by igneous and metamorphic rocks of the Precambrian era. Granite quartzite and migmatite are the major rock types (Egbinola and Amanambu 2014). Usually, the rock types found within this area are regarded as poor aquifers judging by their inherently characterized low permeability and porosity (Egbinola and Amanambu, 2014; Amanambu, 2015). Though, some levels of porosity and permeability are developed through fractures and weathering, which in turn depends on the constituent materials of the parent rock. Therefore, the accessibility of groundwater depends on the weathered material's level and the extent to which joints and fractures are present (Egbinola and Amanambu 2014). The highest groundwater yield in basement terrain is found in areas where thick overburden overlies fracture zones; these zones are often characterized by relatively low resistivity value. The basement aquifers are often limited in extent both laterally and vertically (Olorunfemi and Fasuyi, 1993; Satpathy and Kanugo, 1976). Basement aquifers are developed within the weathered overburden and fractured bedrock of crystalline rocks of intrusive and/or metamorphic origin which are mainly of Precambrian age (Wright, 1992). Hydrogeologically, viable aquifers wholly within the fractured bedrock are of rare occurrence because of the typically low storativity of fracture systems (Clark, 1985). The localized nature of the basement aquifer system makes detail knowledge of the subsurface geology, its extent of weathering and structural disposition through geological and geophysical investigation inevitable.

3.0 MATERIALS AND METHODS

3.1 Theoretical Background of Natural Electric Field (NEF)

The NEF passive electromagnetic method (EM) is used to assess the Earth's conductivity structure across various depths, from a few tens of meters to several hundreds of kilometers. This method measures fluctuations in the natural electric (E)



Figure 1: A Field photograph showing the Study Area (Cassava Processing Site)

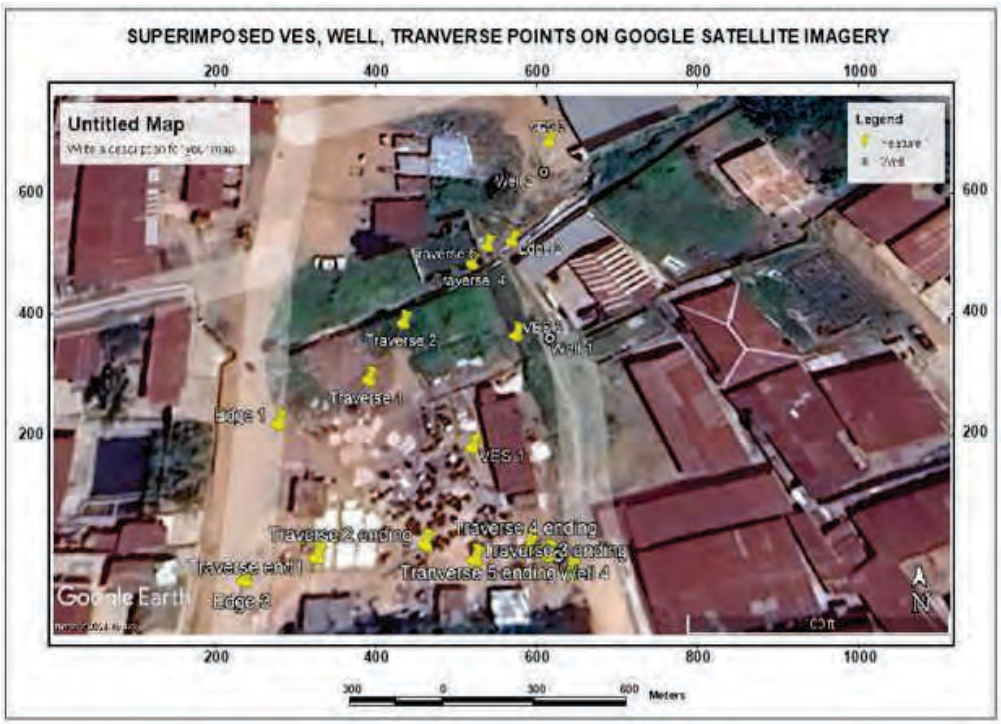


Figure 2: Satellite Map of the Study Area showing the Survey Area and the Profile Lines.

and magnetic (B) fields of geomagnetic disturbances that primarily originate in the ionosphere. The measurements are taken in orthogonal directions at the Earth's surface within the frequency range of 0–30 kHz (Harinath, 2020). The PQWT utilizes three integrated geophysical approaches, including magnetotelluric (MT), induced polarization (IP),

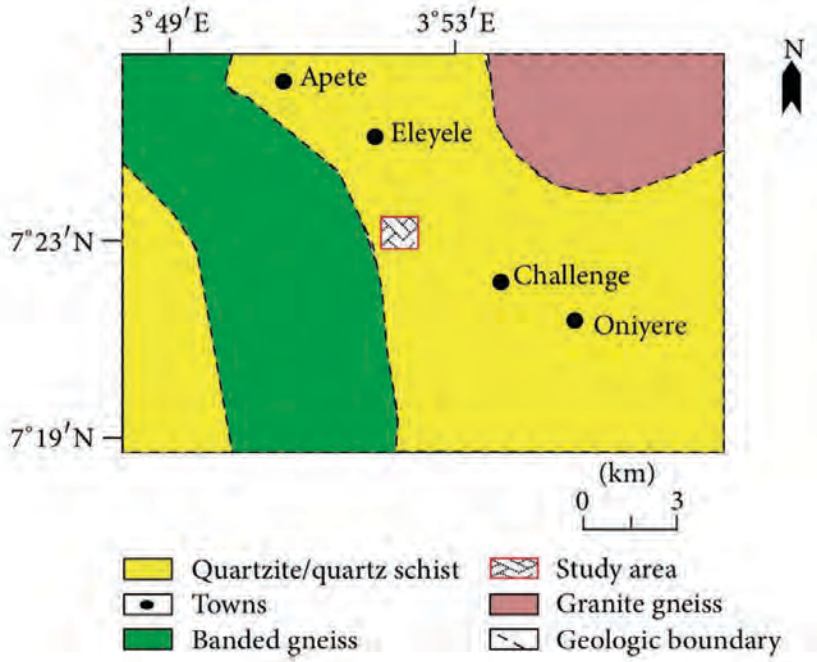


Figure 3: Geology Map of the Study Area (Dare and Fatoba, 2014)

and nuclear magnetic resonance (NMR), to detect subsurface water resources and geological ore deposits (Heiling et al., 2018). The performance of NMR depends on the magnitude of the natural geomagnetic field, the electrical conductivity of rocks and the electromagnetic noise. The earth's steady magnetic field is produced by many sources both above and beneath the earth's surface (Hunan, 2017). The primary source of the field is self –sustaining geodynamo action of the earth's liquid outer core. The geomagnetic dynamo is recognized as the most significant natural field source because all other sources depend on it. In the dynamo mechanism, fluid mechanism, fluid motion in the core moves conducting material across an existing magnetic field and creates an electric current. This current produces a magnetic field that also interacts with the fluid motion to create a secondary magnetic field the same orientation as the original field (Heilig et al., 2018). The PQWT—TC150 multi-channel and multi-functional underground water and leakage detector equipment from Hunan Puqi Geologic Exploration Equipment and Hunan Puqi Water Environment Research Institute Company-Limited, China as described in (Hunan, 2018) and (Alabi et al., 2020), is an automated geophysical prospecting instrument with high sensitivity. It calculates the potential difference between any two ground-based locations and maps resistivity contrasts of groundwater and underground rocks. This is achieved by analyzing the variations in anomalous changes in geological bodies carried by natural electric current of varying frequency electric field components. The PQWT equipment is also referred to as a natural electric field frequency selection system because it uses the natural electric field as the field source (Hunan, 2017). The operation of PQWT—TC150 is based on the observed differences in the conductivity properties of the underground geological structures. It measures the electrical difference of

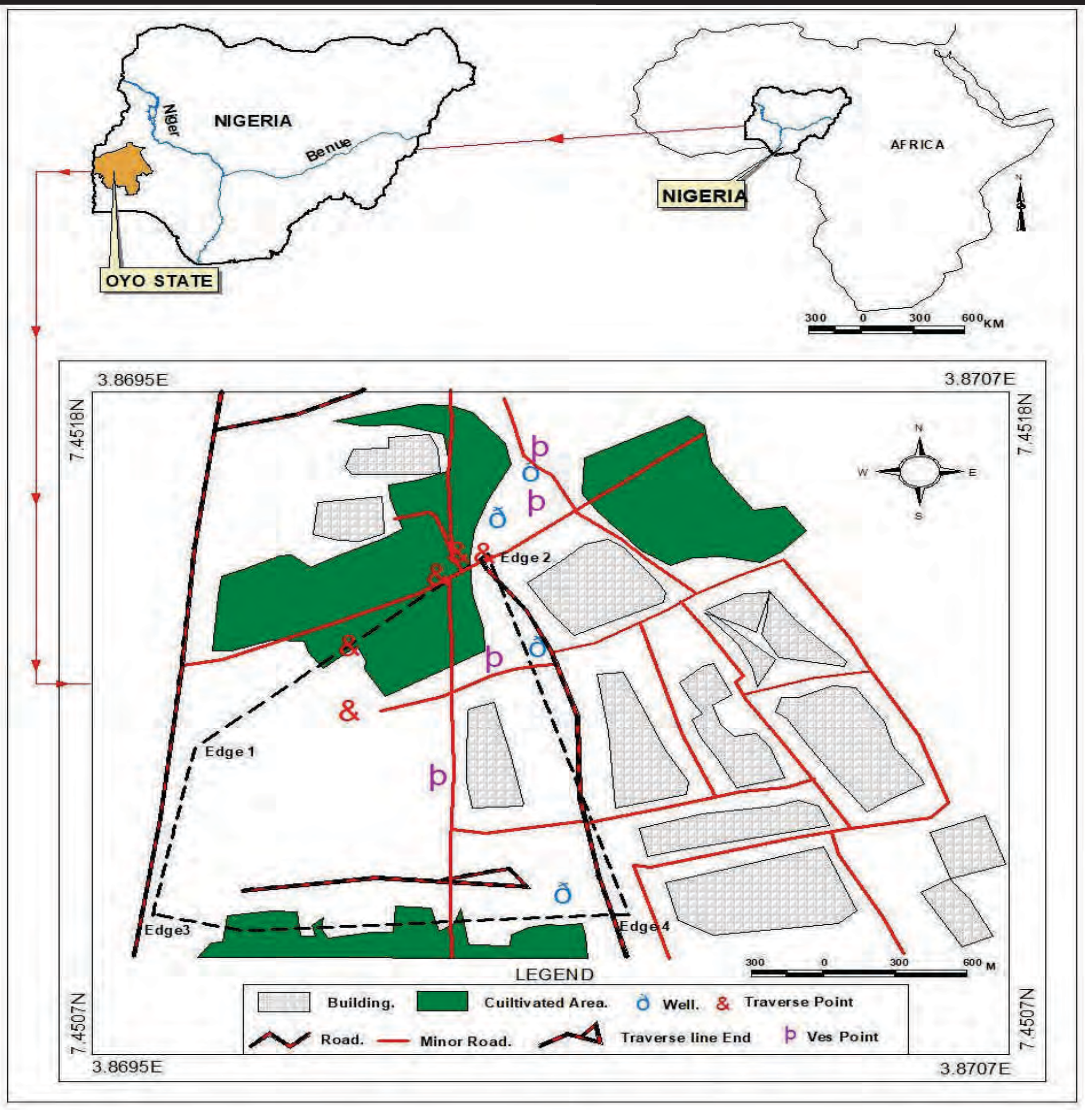


Figure 4: Data Acquisition Map of the Study Area

natural earth magnetic field and their variation at different frequencies and depths. The results obtained from both audio frequency magnetic telluric (ADMT 600S-X) and PQWT equipment have proven to be valuable in real-life applications and have been featured in high-profile research articles. The in-built algorithm of the PQWT is highly efficient, having undergone rigorous testing and validation by esteemed researchers at the Hunan Puqi Geologic Exploration Equipment Institute in China. The PQWT technology has been widely adopted for groundwater exploration and environmental studies. Recent successful applications in groundwater exploration and environmental studies have been reported by (Adagunodo et al., 2023; Legchenko et al., 2002; Hunan, 2017), indicating the reliability and practical significance of the PQWT's in-built algorithm.

The magnetotelluric (MT) method is a passive electromagnetic (EM) exploration method that measures orthogonal components of the electric and magnetic fields on the Earth's surface. The

source field is naturally generated by variations in Earth's magnetic field, which provides a wide and continuous spectrum of EM field waves. These fields induce currents into the Earth, which are measured at the surface and contain information about subsurface resistivity structures unlike controlled-source EM methods which may use an inductive loop as a source; the MT method relies on naturally-occurring electromagnetic fields. The type of natural source depends on the frequency of the EM field and field variation at the Earth's surface. Investigation depth ranges from 100 m below ground by recording higher frequencies down to 200 km or deeper with long-period soundings (Hunan, 2017; Waff, 2000; Guru et al., 2017). The ultraviolet radiation from the sun ionizes molecules of air in the thin upper atmosphere of the earth. The ions accumulate in several layers forming the ionosphere at altitudes between about 80 km and 1500 km above the earth's surface. Electric currents in the ionosphere arise from systematic motions of the ions which are affected by various factors such as the daily and monthly tides, seasonal variations in isolation and the periodic fluctuation is ionization related to the 11 year sunspot cycle (Lowrie, 2007). The currents produce varying magnetic fields with the same frequencies which are observed at the surface of the earth and can be analyzed from long-term continuous records of the geomagnetic field. The ionosphere effects show up in the energy spectrum of the geomagnetic field as distinct peaks representing periods that range from fractions of a second (geomagnetic pulsations) to several years. The magnetic field induces fluctuating electric currents called telluric currents, which flow in horizontal layers in the crust and mantle. The current pattern consists of several huge whorls, thousands of kilometers across which remain fixed with respect to the sun and thus move around the earth as it rotates. The distribution of telluric current density depends on the variation of resistivity in the horizontal conducting layers. At shallow crustal depths the lines of current flow are disturbed by subsurface structures which cause contracts in resistivity. These could arise from geological structures or the presence of mineralized zones. Consider, for example, a buried anticline which has a highly resistive rock (such as granite) as its core and its core and is overlain by a conducting layer of porous sedimentary rocks saturated with groundwater. The horizontal flow of telluric current across the anticline chooses the less-resistive path through the conducting sediments. The current lines bunch together over the axis of the anticline increasing the horizontal current density. The equipotential surfaces normal to the current lines intersect the ground surface where the potential difference can be measured with a high impedance voltmeter (Lowrie, 2007). The field equipment for measuring telluric current density is simple. The sensors are a pair of non-polarizable electrodes with a fixed separation L of the order of 10 to 100m. The potential difference V between the electrodes is measured with a high-impedance voltmeter. The electric field E at a point mid-way between the electrodes can be assumed to be V/L using ohm's law and assuming the telluric current flows in conducting rock layer with resistivity ρ_1 the telluric current density J at each measurement station along a profile is given by

$$J = \frac{V}{\rho_1 L} \quad (1)$$

The direction of the telluric current is not known,

so two pairs of electrodes oriented perpendicular to each other are used. One pair is aligned north-south, the other east-west. Telluric currents vary unpredictably with time but they change only slowly within a homogeneous region. To keep track of the temporal changes, an orthogonal pair of electrodes is set up at a fixed base station outside the area to be explored. Another orthogonal pair is moved across the survey area. The potential difference across each electrode pair in the mobile and base arrays is recorded simultaneously for several minutes at each measurement station; correlation of the records allows removal of the temporal changes in the direction and intensity of the telluric currents. The deflection of telluric current by a resistive subsurface structure is greatly idealized. It assumes an infinite resistivity ρ_2 in the core of the anticline. In practice, the current is not completely diverted through the better-conducting layer; part flows through the more resistive layer as well. Thus, we cannot assume that the resistivity ρ_1 in equation 1.0 corresponds to the good conductor. Rather, it represents some undefined mixture of the value of ρ_1 and ρ_2. It is not the true resistivity of either layer but the apparent resistivity of the measurement (Lowrie, 2007).

The PQWT device adopts a physical phenomenon where nuclei in a strong constant magnetic field are perturbed by a weak oscillating magnetic field and respond by producing an electromagnetic signal with a frequency characteristic of the magnetic field. In nuclear magnetic resonance and related techniques, an electromagnetic signal with a frequency characteristic of the magnetic field is detected from nuclei that have a nuclear magnetic moment and a non-zero spin; these are typically nuclei with an odd number of protons or neutrons (Legchenko, 2002). This process occurs near resonance when the oscillation frequency matches the intrinsic frequency of the nuclei. This is however dependent on the strength of the static magnetic field, the chemical environment and the magnetic properties of the isotope involved (Legchenko, 2002; Alabi *et al*., 2022). Conventionally, radiations from the earth that originates from the rock minerals, ore bodies, subsurface water or other geological structures are affected by a magnetic or electric field and when these radioactive emissions pass through a magnetic field or charged plates, they disintegrate into alpha particles, beta particles and gamma rays. The gamma rays are electromagnetic waves with no charge, and it remains undeflected through the field. This is the actual phenomenon that produces the natural electromagnetic field whose electric field component can be measured to determine the resistivity properties of the originating material in the subsurface. The variations in the frequencies of the electromagnetic field in the subsurface ranging from 0.30 kHz are thus incorporated by PQWT-TC150 to study the underground field for the imposing geological challenges (Harinath, 2020). The NEF survey by PQWT-TC150 involves the passive measurement of the electric E and the magnetic B fields in an orthogonal direction at the ground surface of the earth with two non-polarizable potential electrodes. The geomagnetic field is regarded as a plane wave whose distribution is perpendicular to the ground and is distributed far from the field source. The ratio of horizontal electric field component (*Ex*) and the magnitudes of the magnetic field component (*Hy*) are measured in the time/frequency domain and are consequently utilized in computing the resistivity structure of subsurface by the PQWT equipment. The apparent resistivity of the medium under interaction is derived by substituting electric and magnetic field

components in Cagniard's scalar resistivity formulae resulting in equation 2.0 (Cagniard, 1953; Waff, 2000).

$$\rho m = 1(5f)^{-1}\left(\frac{E_x}{E_y}\right)^2 \quad (2)$$

The resistivity of the medium under contact is represented by ρm, the operating frequency is denoted by f respectively, *Ex* and *Hy* are the electric field component and magnetic field component of the field respectively. Equation 2 as reported by (Waff, 2000), is the result of inserting the electric and magnetic field components, as described by (Adeniji *et al.*, 2024) in Cagniard's scalar resistivity formulas to obtain the apparent resistivity of the medium under interaction. Consequently, the electric field component interacts with the ground perpendicularly, while the magnetic component of the field is assumed to remain constant. The depth of penetration (δ) of a plane electromagnetic waves propagated on the ground according to attenuation characteristics is given in equation 3.0. The geologic properties of the material under contact may be ascertained from the qualitative connection between the resistivity of the ground under interaction and the electric field component. Equation 3 indicates that the penetrating depth of electromagnetic waves in a medium is directly proportional to the resistivity of the medium at a constant frequency.

$$\delta = 503.3\sqrt{\frac{\rho}{f}} \quad (3)$$

Then, using Equation 3.0 and the Maxwell electromagnetic theory under the assumptions that the ground is homogeneous, isotropic, and horizontally layered (Rensburg, 2019). The effects of the displacement current where *Ex* and *Hy* fall between the π/2 phase angles are likewise ignored, implying that the data collection lines are perpendicular to the subsurface structure (Rensburg, 2019; Alabi et al., 2022). This serves as a premise on which magnetic field is considered as a constant function of the electric field response across a narrow region of measurement and is stable in most circumstances. Moreso, magnetotellurics procedure is part for which the PQWT-TC150 operations as reported is because the magnetic field is stable in most scenarios and is regarded as a constant function of the electric field response over a small area of measurement (Zonge and Hughes, 1991, Alabi et al., 2022). According to (Hunan, 2018), the electric components of the earth's electromagnetic field at different frequencies are measured in millivolts (mV) to estimate the resistivity contrast of the different geologic structures with regard to the lithological bodies under contact under the field layout displayed in figure 5.

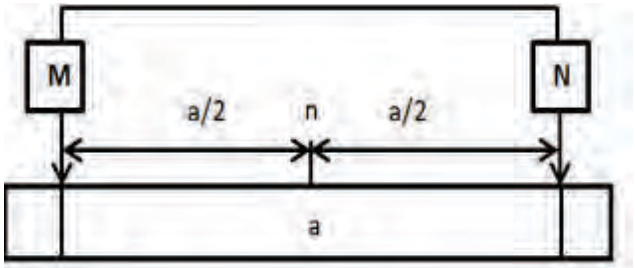


Figure 5: Sketch of the PQWT Survey showing the full electrode spacing (a) and half electrode spacing (a⁄2) (Hunan, 2018)

The significance of convergence points (C) on the 1D model and their corresponding features on the 2D model, particularly about identifying fluid-filled mediums or layers with low resistivity, is from the relationship between the wavelength and the frequency, such that.

$$f = \frac{c}{\lambda} \quad (4)$$

If the frequency of an EM wave is known (which was presented in frequency curve maps), the wavelength can be easily determined, since all EM waves travel at the speed of light, where *f* is frequency, λ is the wavelength, and c is the speed of light. Therefore, a point of convergence (which

is represented as c) of electrical potential difference (in mV) curves at varying frequencies on the 1D model corresponds to a porous medium filled with fluid or a weathered rock formation (Adagunodo *et al.*, 2023). Meanwhile, a high divergence of electrical potential difference curves could indicate a highly resistive, highly compacted, or hard rock terrain. In EM prospecting, the penetration depth depends on the stratum's electrical conductivity and the frequency at which the EM field propagates (Adagunodo *et al*., 2023). The amplitude of the EM field decreases exponentially as it penetrates the subsurface, which in turn increases the penetration depth as the EM frequency and the conductivity of the stratum decrease (Adagunodo *et al*., 2023). The magnetotelluric geophysical method is the Earth's electromagnetic field in millivolt (mV) on the vertical axis and lateral sampling distance on the horizontal axis.

3.2 Field Data Acquisition and Analysis

The NEF field measurement was undertaken by placing the two potential electrodes at points N and M extended 10m apart on the ground for the purpose of taking the first reading on each of the investigated traverse (Figure 7 and 8). A total of five electromagnetic (EM) traverses including four traverses (NEFT1-NEFT4) was conducted using PQWT−TC150 equipment probing varying depths of up to 150 m while the fifth traverse (NEFT5) was adopted as a controlled site at a distance of 500m away from the study area. A console cable was used to connect the probes to the instrument which determines the electromagnetic impulses that have been generated by the aforementioned points and the generated data were automatically saved on the instrument. The actual position of N and M electrodes and their corresponding spaces are displayed in Figure 5. The N and M electrodes were consequently moved 5m progressively on the traverse line implying that N was moved to 5 m, while M was moved 15m to take up the next reading with the electrode change in position M to M1 and N to N1 respectively indicated with blue and red colours (Figure 6). The copper electrodes were connected to the electrode cables of the PQWT equipment, and subsequently linked to an LCD touch-screen for the display of probing depth, subsurface water imagery, and infiltration levels. The number of sound points per traverse ranged from 5 points in traverse 5 to 16 points corresponding to 25m to 80m in traverse 4. A visual representation of the PQWT Survey as illustrated in (Figure 6) NEF data were acquired using an inter-data point interval of 5m within the study area with four (4) traverses within the site which covers about 0.17327 km2 and one (1) traverse (NEFT 5) outside the site; at a distance of 500m south of the cassava processing site consequently marked as control site. The positions of the Probes M and N were at distances of 0m and 10m from the ground, are in accordance with published literature as documented by Oyegoke *et al*. (2020), Alabi *et al.*, 2022 and Gomo (2023). These probes were linked to the EM console via cable to capture the EM impulse generated by the respective points. These processes were thus followed until the entire length of the traverse is completed. The electrical potential differences between the pairs of the electrodes in contact with the ground are the primary data captured at different stations on each of the five traverses in the study area. The instrument at the push of a button measures the

electric field component of thirty-six different frequencies in the geomagnetic field in millivolt (mV) and a frequency curve with identified profile map was generated at the display of the PQWT-TC150 from the acquired data as processed and analyzed by MATLAB mathematical package. The frequency curve displayed how the normal frequency lines within the subsurface respond to the application of a small change in potential difference in millivolt by the instrument (Hunan, 2017; Alabi et al., 2022). A straight frequency line reveals a homogeneous subsurface material while a curvy or angular line indicates variations in subsurface rock properties. The algorithm on the PQWT-TC150 was computed with equation 2 and 3 in order to maximize the electric field response in mV to generate a profile map with a resistance bar usually displayed at the right-hand side of the map from red at the top to blue at the base (Keary, 2002; Hunan, 2017). The regions associated with red coloured scheme in the NEF profile maps (Figure 10, 12, 14, 16 and 18) indicate the highly resistive zones, and as the colour spectrum migrates towards the blue colour the resistance gradually diminishes. Regions with a high tendency for groundwater were identified with blue colour on the profile map, fractures and faults are well noticeable where typical contour lines were concentrated while regions that were concentrated with very deep colourations are highly conductive area that must have been significantly impacted by a contamination plume and are consequently targeted as contaminated zones (Hunan, 2017; Hunan, 2018; Alabi *et al.*, 2022). Since the natural electric current within the subsurface is a resultant effect of electrochemical processes among conductive minerals and fluid contents in porous media, the earth's electromagnetic field (E-field) component, measured in millivolts at various frequencies, is therefore instrumental in determining the resistivity contrast of different geologic bodies about the near-surface lithological units, as reported by Adagunodo *et al.* (2023).

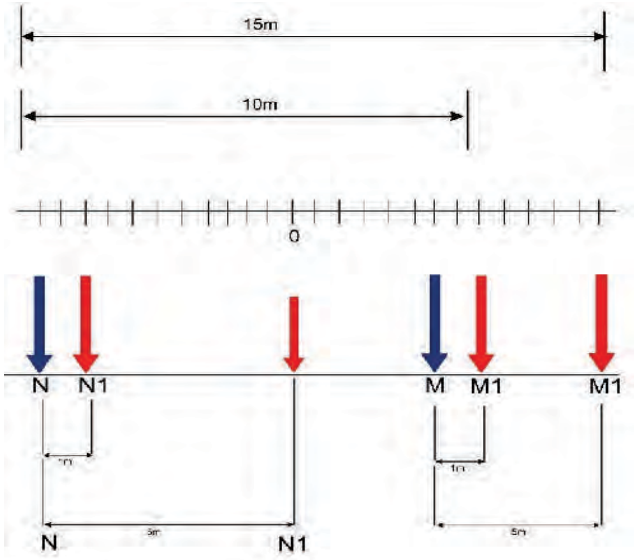


Figure 6: Field Set-up for NEFT survey using PQWT Equipment and Electrode Configuration.

4.0 RESULTS AND DISCUSSION

The comprehensive analysis of the collected natural electric field data and output from the internal algorithm within the PQWT−TC150 equipment used for the measurement yielded a frequency curve and a profile map, illustrating the variation in the electric potential difference (EPD) across each traverse. The generated frequency curve is a plot of thirty–six frequency responses of the earth's electromagnetic field in millivolt (mV) on the vertical axis and the lateral sampling distance on the horizontal axis each of the five (5) selected traverses. The corresponding profile maps provide the pictorial interpretation of the frequency response of the subsurface to a depth of 150m. The corresponding profile maps provide

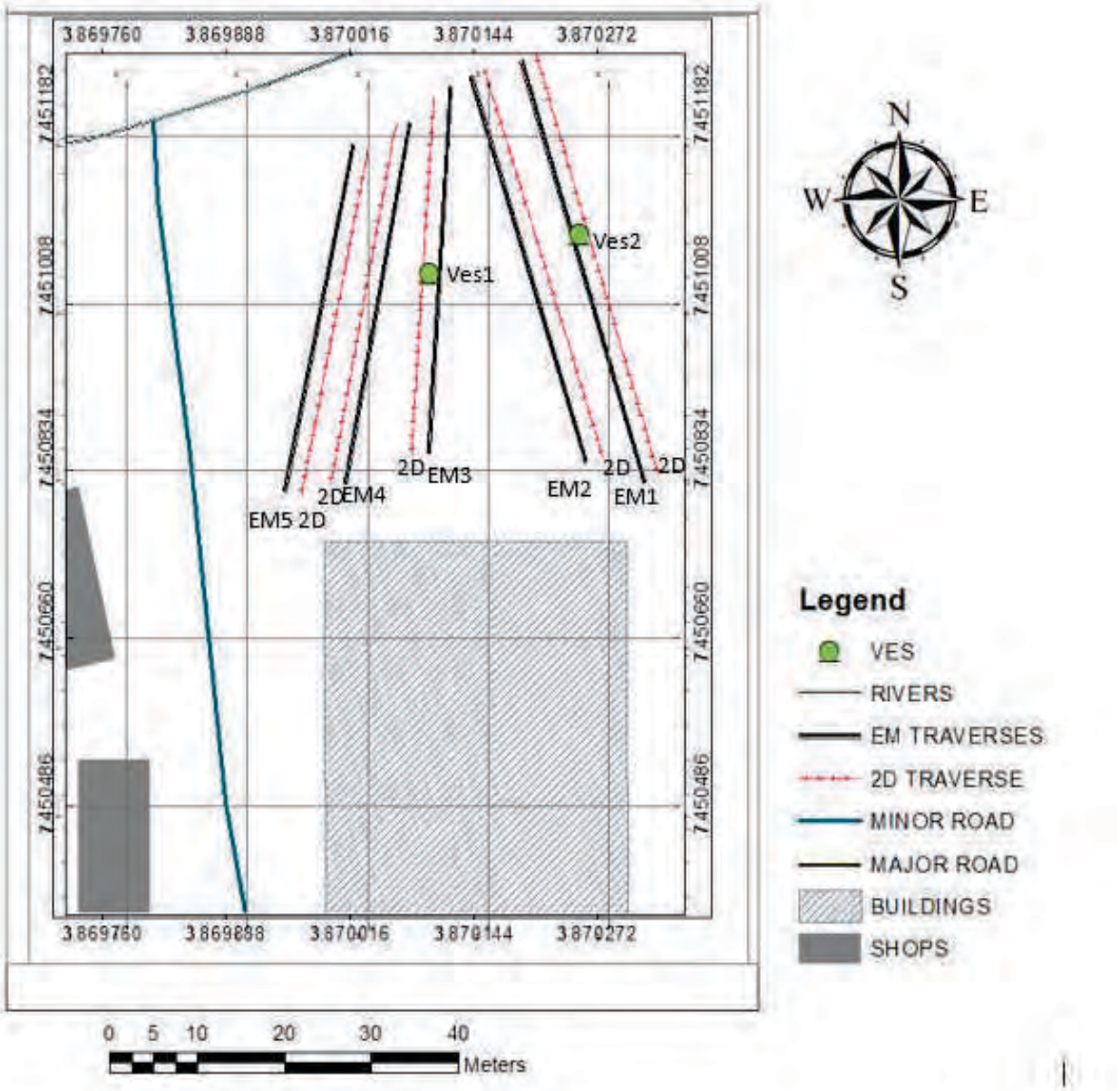


Figure 7: Basemap showing the Data Location Points in the Study Area

the pictorial interpretation of the frequency response of the subsurface to a depth of 150 m. The vertical axis reveals the depth into the subsurface and the horizontal axis gives the lateral distance covered. The frequency response is used to map the contour lines on the profile map and the regions where the lines concentrate or diverge reveal the presence of a significant anomaly. The frequency curve represents the electric potential difference plotted against profile distance, while the profile map provides a subsurface representation of the electric potential difference relative to depth and profile distance. Notably, points of convergence (c) or areas exhibiting very low EPD signals on the frequency curve corresponding to regions characterized by low resistivity on the profile map were identified, imaging different delineated various subsurface features; zones of weathered basement, polluted aquifers among others while the regions



Figure 8: An Image showing the Electromagnetic Instrument (PQWT) in the Field.

associated with leachates were delineated from non-contaminated areas. The vertical axis shows the depth into the subsurface and the horizontal axis gives the lateral distance covered. The frequency response is used to map the contour line on the profile map and the region where the line concentrates or diverges reveals the presence of a significant anomaly of leachates. The corresponding profile maps provide the image interpretation of the frequency response of the subsurface to a depth of 150 m. The vertical axis shows the depth into the subsurface and the horizontal axis gives the lateral distance covered. The frequency response is used to map the contour line on the profile map and the region where the line concentrates or diverges reveals the presence of a significant anomaly of leachates.

The frequency curves from traverse one (NEFT1) shows a peak potential response of 4.1 mV along the traverse, representing the normal frequency response at the station. The normal frequency lines show some distinct curvy responses at stations 3-5 and 7-10 and across the whole length of the profile. The curvy responses were in turn interpreted in the 2D geo-section of the profile map as a contaminated zone between station 2 (10 m), 3−5 (15 m – 25 m) and 7−10 (35m − 50 m) at depths of 10 m, 15 m and 40 m respectively (Figure 9 and 10). The 2D geo-section of the magnetotelluric survey reveals the extent of



I	N	Freq 01	Freq 02	Freq 03	Freq 04	Freq 05	Freq 06	Freq 07	Freq 08	Freq 09	Freq 10	Freq 11	Freq 12	Freq 13	Freq 14	Freq 15	Freq 16	Freq 17	Freq 18	Freq 19	Freq 20
185	1	0	0	0	0.283	0.281	0.32	0.223	0.223	0.221	0.251	0.036	0.212	0.273	0.283	0.273	0.366	0.34	0.378	1.726	1.899
185	2	0.20	0.185	0.247	0.255	0.253	0.26	0.233	0.223	0.274	0.249	0.254	0.243	0.366	0.297	0.366	0.587	1.743	1.829	1985	2192
185	3	0.04	0.02	0.426	0.416	0.416	0.34	0.387	0.387	0.392	0.376	0.316	0.276	0.328	0.307	0.328	0.326	0.321	0.321	0371	1743
185	4	0	0	0	0	0	0.26	0.223	0.223	0.351	0.319	0.255	0.349	0.328	0.292	0.328	0.326	0.395	0.395	1.709	2002

Figure 9: Frequency Curve for Apete Traverse 1

leachate migration in the soil. The figure-interpreted traverse distinguishes different geological strata based on variations in electric properties such as resistivity and potential difference. The traverse can be divided into four distinct zones or layers, as illustrated in Figure 10. The result of NEF measurement along traverse 1 (NEFT1) trends from west to east orientation with a total length of 50m which matches 10 data points with convergence (c) points on the frequency curve and linear streamline of electric potential difference curves towards the top. These two features correspond to a concentrated conductive medium being observed on the profile map varying from the surface to a depth of 32m (Figure 10). Zone 1 being the top layer is predominantly affected by leachates and therefore served as the conductive zone with recognizable blue colour. It extends from the surface to depths ranging from 5 to 15 m at stations 1 and 2, 5 to 18 m at station 4, and up to 30 m at station 7, which is significantly impacted by a contamination plume. Additionally, at station 9, the depth of this zone reaches 30 to 35 m. This zone indicates that the primary contaminant leachate plume is present in high quantities within the structure; spread around it is another low resistive layer. Zone 2 represented in green on the legend, follows the leachate-affected zone. The potential difference value range in this zone ranged from 0.40 to 0.52 mV, which is somewhat elevated. This layer is partially affected by the leachate plume. These layers were underlain by subsequent higher resistive layers up to about 75 m, the rest of the subsurface from 75 m to where the investigation covered possessed higher resistance property as displayed in the contour lines in the 2D geo-section of the profile map; zones 3 and 4 showed no significant impact

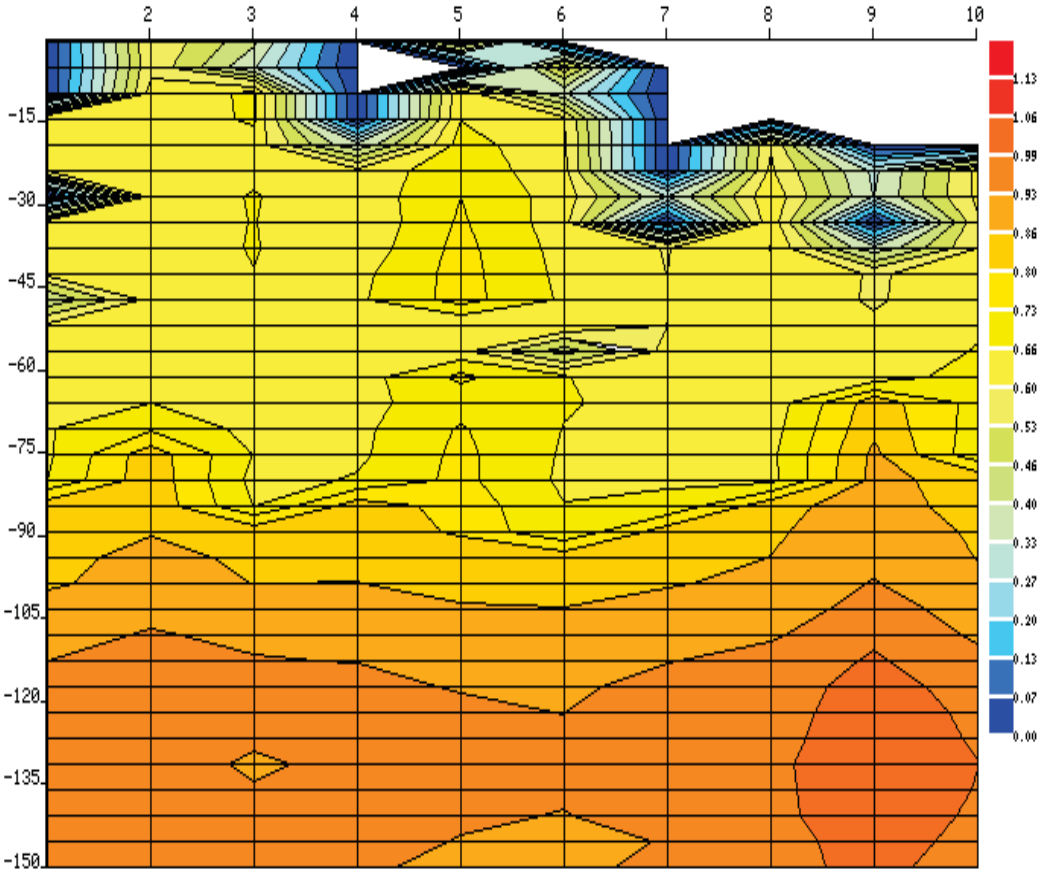
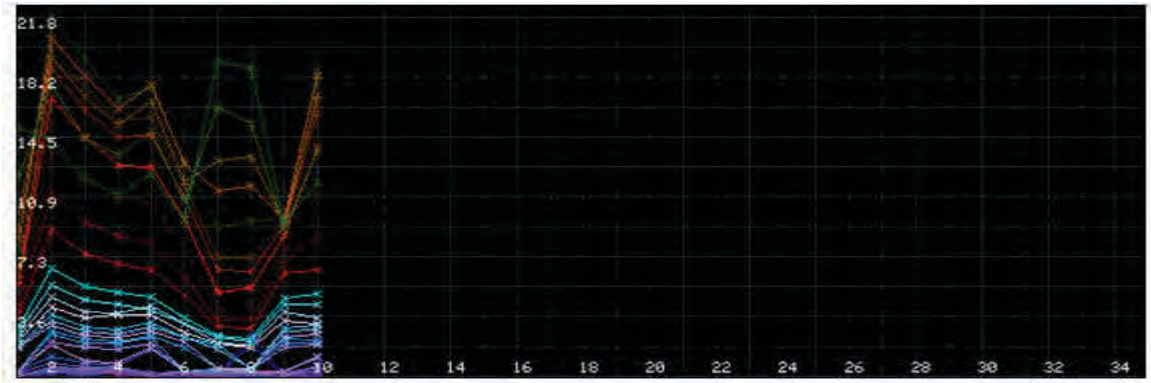


Figure 10: NEF-Profile Map for Apete Traverse 1

from the leachate plume and no noticeable influence from waste-generated leachates within these zones. Therefore, the conductive media are interpreted as being saturated with leachates at the topsoil to the depth of 40 m with depth ranging along the 2D geo-section of the profile map. The layers beneath the leachates are interpreted as weathered terrain and fresh basement, respectively. Groundwater from the shallow hand-dug well (< 5 m deep) around traverse 1 is unfit for domestic usage, due to the depth of infiltration of leachate contaminants.

The second traverse (NEFT2) has a peak potential response of 21.8 mV at station 2 of the traverse alongside other sharp variations of about 18.2, 19.5, 18.7 and 18.2 respectively represented at stations 5 (25 m), 7 (35 m), 8 (40 m) and 10 (50 m). The lateral distance of the traverse line has a length of 50m with 10 data points. Several convergence (c) points are present with stream-lined curves on the frequency model as shown in Figure 11. These observed responses were interpreted in the 2D geo-section of the profile map as a vertical fracture with entrapment of contaminant plumes of low resistive signatures ranging from 0.0 to 0.08 mV (higher conductivities) spreading from station 7 to 10 at lateral distance of 35m to 50m (Figure 10b)(Carpenter and Ready, 2011). The contaminated zone was centered at station 2 (10 m) at intercepted intervals surrounded by low resistive section down to the depth of 35m (blue colour). The 2D geo-section reveals four distinct



I	N	Freq 01	Freq 02	Freq 03	Freq 04	Freq 05	Freq 06	Freq 07	Freq 08	Freq 09	Freq 10	Freq 11	Freq 12	Freq 13	Freq 14	Freq 15	Freq 16	Freq 17	Freq 18	Freq 19	Freq 20
186	1	0	0	0	0	0	0.02	0.019	0.022	0.022	0.226	0.292	0.318	0.366	0.425	0.44	1.778	1.881	1.995	2.226	2.451
186	2	0.26	0.28	0.276	0.255	0.371	0.41	0.381	0.476	0.571	0.847	1.212	1.916	2.175	2.572	2.796	3.176	3.400	3.745	4.263	4.884
186	3	0.17	0.21	0.206	0.292	0.245	0.32	0.400	0.419	0.478	0.563	0.855	0.937	1.812	2.088	2.33	2.521	2.761	3.982	3.555	3.987
186	4	0.19	0.30	0.299	0.340	0.361	0.42	0.385	0.589	0.582	0.557	0.654	0.854	1.776	2.088	2.175	2.365	2.589	2.865	3.814	3.901
186	5	0	0.19	0	0	0.185	0	0	0	0.019	0.188	0.779	1.778	2.088	2.434	2.468	2.744	3.003	3.297	3.745	4.281
186	6	0.29	0.20	0.319	0.266	0.198	0.02	0.022	0.271	0.245	0.295	0.340	0.309	0.297	0.352	1.761	2.123	2.434	2.399	2.641	3.227
186	7	0	0	0	0	0	0.02	0.178	0.212	0.233	0.288	0.352	0.381	0.421	0.475	0.485	0.53	1.726	1.916	2.802	2.037
186	8	0	0	1.985	2.498	0	0	0.178	0.021	0.147	0.25	0.321	0.340	0.380	0.433	0.463	0.487	0.511	0.535	1.795	1.951
186	9	0	0.18	0	0	0.183	0	0	0	0.017	0.25	0.290	0.278	1.743	2.088	2.295	2.416	2.761	2.951	3.417	3.972
186	10	0.02	0.33	0.195	0.264	0.328	0.45	0.549	0.614	0.614	0.621	1.110	1.222	1.916	2.071	2.244	2.554	2.848	3.176	3.262	3.607

Figure 11: Frequency Curve for Apete Traverse 2

layers. The first layer indicates stations affected by the leachate plume including Stations 1, 5, 7, 9 and 10. These stations were influenced by the plume at depths ranging from 0 to 15 m, 0 to 38 m, 0 to 28 m, and 5 to 40 m respectively. The underlying layer also exhibited low resistive signature to an average depth of 75 m conspicuously observed in station 8 (40 m). The rest of the subsurface down to the depth of 150 m were characterized by higher resistance value with varying displayed lines of contour signature (Figure 12). It was observed that leachate contaminants have infiltrated to about 45 m depth as shown in Figure 12. Most of the identified zones for groundwater developments at station 5 to 10 (25 m to 50 m) are associated with high yields due to the very high pattern of the conductive media; the rock contacts in these locations could have been the most viable spot for borehole drilling but could also serve as collecting troughs for leachate accumulations and migrations, which has made the spot unsuitable for drilling.

Traverse 3 exhibited the highest peak potential response of 40.1mV amidst all the five (5) investigated traverse lines in the study area. This was observed at station 5(25 m) alongside station 3(15 m) while other. Other stations displayed minimal range of peak potential response variation with 1, 2, 3 and 4 converging around 23.0, 21.0, 25.0 and 23.0 mV respectively. The frequency responses were observed to converge largely between stations 1 to 4 which is revealed in the interpreted 2D geo-section of the profile map to be a highly resistive region denoted with blue colour (Figure 13). The top layer is relatively constant on the resistance scale to an average depth of 20m below the surface and the same material is observed to vertically extend deeper

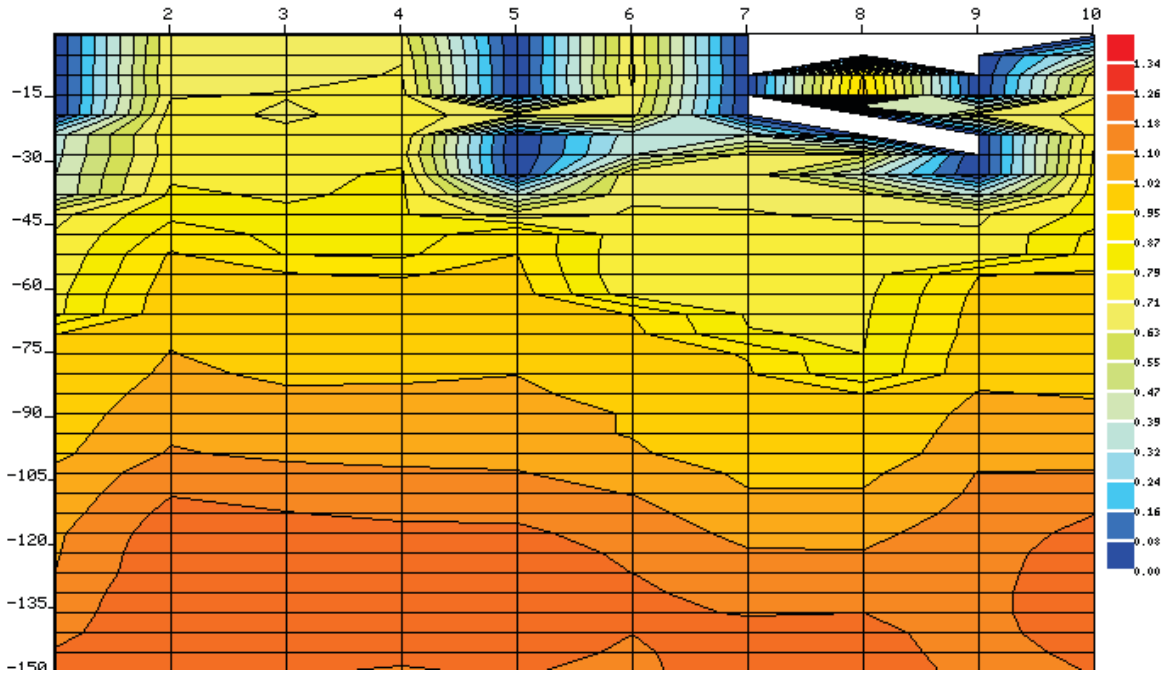
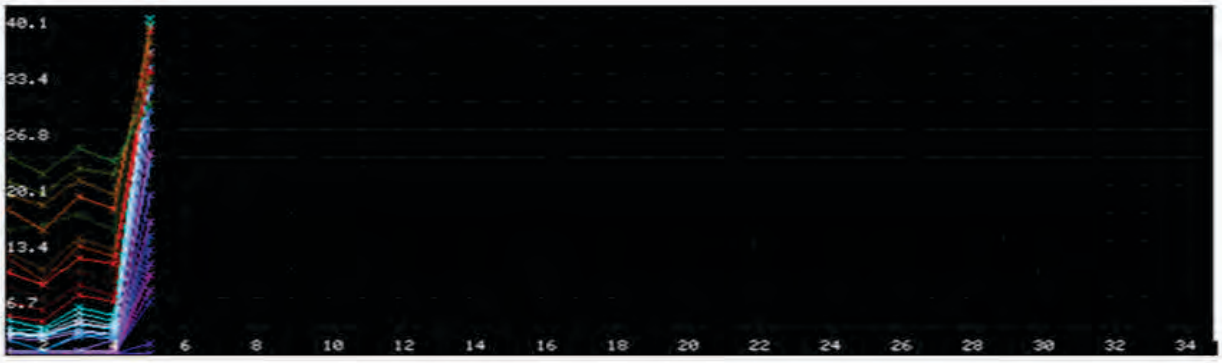


Figure 12: NEF- Profile Map for Apete Traverse 2

into the subsurface between stations 1 to 4 across the profile. Large varying contour lines indicating vertically fractured zone was observed at station 4 to 5 towards the end of the traverse line at depths of 10 m to 20 m. The 2D geo-section of the interpreted profile map does not reveal any pocket fractures across the traverse line except in station 4 to 5 with lateral distance of 20 m to 25 m at depths of 5 m to 15 m but higher resistance layers were gradually encountered down to the depth of 150m (Figure 14). the resistance of the media across the traverse length though, seemingly inhomogeneous, the variation below the surface is closely at a higher potential value The observed color variation effectively highlights the varying zones of electrical conductivity, thereby revealing the extent of the leachate plume within the study area. The map categorizes the area into three distinct layers. The first layer indicates the presence of leachate, which extends across the entire map from the left flank to the right flank. The depth of leachate ranges from 15 to 30 m at Stations 1 through 4, with Station 5 showing pollution from 0 to 30 m. The second layer reveals a contrast in conductivity, though no leachate plume is evident in this layer. Similarly, the final layer shows the signature of a fresh basement, as depicted in Figure 14 and the NEF measurement result of traverse 3 (NEFT3) trends from West to East orientation. In this result, a total of 5 data points, culminating to a profile length of 20 m was covered. The leachate's depths varied from about 15m (at the West) to a depth < 30 m at the East (Figure 11b).

The frequency curve generated from the fourth traverse (NEFT4) measurement possessed a peak potential response of 2.5 mV at station 14 with lateral distance of 70 m (Figure 15). Distinct variations from the normal frequency lines were observed at 2 to 4; 8 to 10; 10 to 16 with corresponding peak potential responses of 2.3 mV, 0.8 mV, 2.5 mV and these were consequently on the 2D geo-section on the profile map as material



I	N	Freq 01	Freq 02	Freq 03	Freq 04	Freq 05	Freq 06	Freq 07	Freq 08	Freq 09	Freq 10	Freq 11	Freq 12	Freq 13	Freq 14	Freq 15	Freq 16
237	1	0	0	0	0	0.083	0.013	0.186	0.211	0.233	0.295	0.349	0.380	0.399	1.829	1.778	1968
237	2	0	0	0	0	0.003	0.019	0.186	0.216	0.233	0.283	0.335	0.362	0.414	0.449	6.46	1726
237	3	0	0	0	0	0.003	0.185	0.200	0.223	0.249	0.364	0.349	0.378	0.411	2.106	2.355	2606
237	4	0	0	0	0	0.003	0.179	0.198	0.221	0.247	0.297	0.347	0.375	1.778	1.933	2..088	23447
237	5	6231	7525	0	1236	951	10.839	12.427	14.17	15.879	19.037	22.886	23939	26.976	29.22	31.464	31912

Figure 13: Frequency Curve for Apete Traverse 3

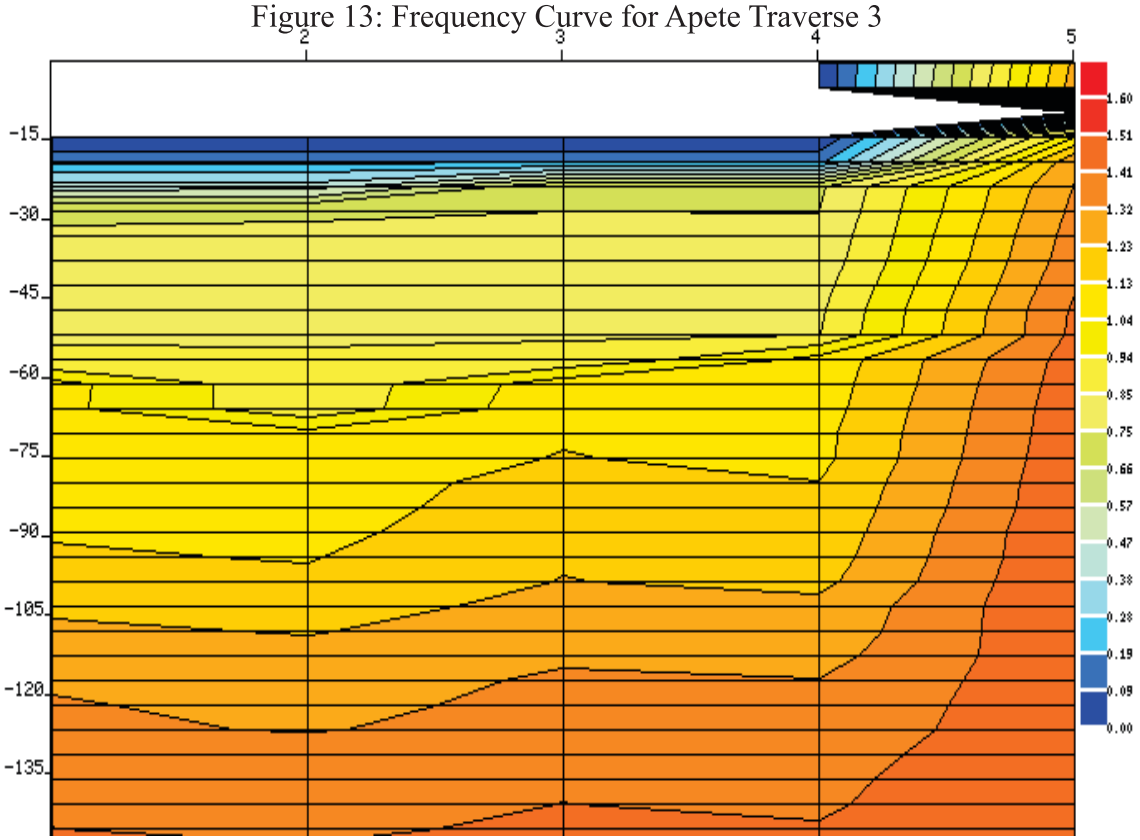


Figure 14: NEF-Profile Map for Apete Traverse 3

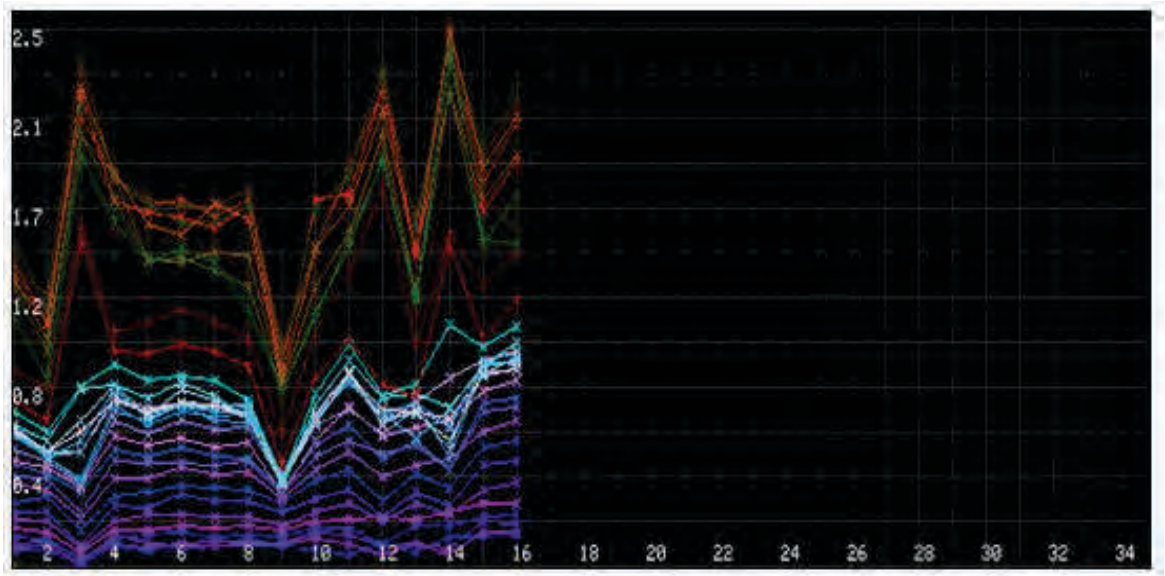
media that were prone to fractures (Figure 16). The NEFT4 measurement result trends from west to east direction. It has a total length of 32m corresponding to 16 data points. The convergence (c) points in Figure 12a corresponding to conductive zones, which are interpreted as

aquifer. Zones of very low resistance were noticeable at station 2 to 4 (10 m to 20 m); 5 to 6 (5 m to 30 m) and 11 to 15 (55 m to 75 m). Four distinct layers were identified with traverse 4 at station 2 to 4 (10 m to 20 m) at depth 25 m, 11 to 13 (55m to 65 m) at depth 8 m, and 14 (70 m) at depth 10 m; these layers were inferred to be associated with contaminant plumes. The first layer is underlain by another low resistive layers spreading across the traverse at a lateral distance up to 45m, which is randomly affected by the leachate plume as observed in Figure 16. The third layer exhibited uniform anomalies with higher resistance ranging from 0.13 to 0.20 mV on the resistance scale at the depths of 30m to 105m observed at station 9 with a depth ranging from 0 to 105m and increased in intensity in station 10 to higher resistance of 0.28 mV to the lateral distance of 16m (Figure 16). Beneath these layers were other layers exhibiting higher resistance down to the depth of 150m with varying displayed lines of contour signatures where further regions become increasingly inhomogeneous. A significant contrast in conductivity is inferred on the right-hand side of the map, where Stations 11 through 14 were impacted by the leachate plume principally in layer 1 alongside layer 2. The second layer is less affected by the plume. Both the third and fourth layers were free from leachate plumes. In this result, the average extent of downward flow of leachates is about 30m from the surface as shown in Figure 16. However, to exploit viable aquifer with uncontaminated water in NEFT4, it is advisable to drill to about 45 m, 40 m−60 m and 40−90m at distance 6−10m, 12m−20m and 22 m−32 m which correspond to data points 3−5, 6−10 and 11−16, respectively. Beneath the leachates medium lies the partly weathered bedrock, which could be interpreted as the migmatite-gneiss complex being the major source rock in the study area (Adejumo, 2018). The result of NEFT4 also revealed aquifer contamination zones at depth 30 m and 25 m respectively toward the west and east direction due to the distribution of leachates.

The frequency curve generated from the fifth traverse (NEFT5) possessed a peak potential response of 15.8 mV at station 8 (40 m). The frequency responses were observed to converge largely between stations 2 to 7 which the interpreted 2D geo-section on the profile map revealed to be a highly resistive region (Figure 17). The potential response dropped from 2.5 mV at station 4, 9 and 11 revealing a highly fractured zone with lower resistance. The top layer was found to be relatively constant on the resistance scale up to the depth of 5 m below the surface and the same subsurface material is observed to be vertically extended deeper into the subsurface between stations 5 to 8 (25 m to 40 m). The result of NEFT5 revealed three distinct layers. However, the entire traverse did not show any detectable trace of a leachate concentration throughout the section to the depth of 150 m. The NEF measurement along traverse 5 (NEFT5) trends from West to East direction, with a total length of 26 m corresponding to 13 data points at a lateral distance of 65 m as shown in Figure 17. The location and direction of traverse 5 is at 500 m away from the cassava-effluent site to the south, which acted as the control profile. The 2D geo-section of the interpreted profile map also reveals separate fracture zones with large varying lines of contour closures indicating vertically fractured zones conspicuously observed at stations 2 (10 m)

to 4 (20 m) at depth 20 m to 30 m; 3 (15 m) to 5 (25 m) at depth of 35 m to 40 m; station 9(45 m) to 10(50 m) at depths 10 m to 20 m and 130 m to 140 m (Figure 18). The 2D geo-section of the profile map indicated that there were no clear potential difference signatures to classify the identified layers as polluted.

Based on the findings of this study considering the five separate investigated traverses (NEFT1 to NEFT5) with the adopted geophysical technique in relation to the impact of CMEs on the subsurface most significantly the groundwater system has revealed that the sanitary integrity and wholesome quality of groundwater and its development in the study area may have been invaded by leachate contamination. The work of Okpoli (2013) and Badmus et al., (2022) revealed much earlier that groundwater contamination from leachate is caused by high-conductivity



I	N	Freq 01	Freq 02	Freq 03	Freq 04	Freq 05	Freq 06	Freq 07	Freq 08	Freq 09	Freq 10	Freq 11	Freq 12	Freq 13	Freq 14	Freq 15
188	1	0.311	0.319	0.342	0.373	0.411	0.454	0.487	0.526	0.616	0.652	0.715	0.725	0.778	0.842	0.835
188	2	0.311	0.326	0.345	0.356	0.392	0.447	0.488	0.559	0.590	0.642	0.664	0.687	0.721	0.744	0.746
188	3	0.231	0.243	0.262	0.266	0.297	0.314	0.333	0.406	0.456	0.488	0.575	0.599	0.609	0.623	0.637
188	4	0.324	0.378	0.342	0.359	0.400	0.445	0.516	0.556	0.635	0.718	0.771	0.834	0.908	0.953	0.984
188	5	0.305	0.337	0.318	0.378	0.397	0.469	0.506	0.582	0.637	0.708	0.744	0.792	0.841	0.903	0.889
188	6	0.311	0.328	0.338	0.395	0.425	0.473	0.563	0.611	0.689	0.715	0.782	0.825	0.904	0.977	0.951
188	7	0.324	0.326	0.350	0.373	0.412	0.468	0.533	0.602	0.661	0.702	0.747	0.785	0.865	0.906	0.934
188	8	0.324	0.335	0.354	0.378	0.421	0.459	0.533	0.589	0.671	0.721	0.735	0.801	0.873	0.894	0.939
188	9	0.331	0.337	0.337	0.373	0.404	0.418	0.485	0.525	0.542	0.568	0.589	0.563	0.623	0.647	0.643
188	10	0.313	0.362	0.388	0.412	0.442	0.487	0.545	0.632	0.677	0.741	0.794	0.825	0.891	0.908	0.932
188	11	0.292	0.342	0.378	0.414	0.451	0.526	0.589	0.683	0.759	0.813	0.882	0.967	0.961	1.111	1.094
188	12	0.337	0.268	0.328	0.342	0.466	0.445	0.454	0.532	0.647	0.751	0.735	0.839	0.842	0.922	0.941
188	13	0.293	0.337	0.340	0.421	0.451	0.528	0.573	0.663	0.704	0.792	0.816	0.884	0.963	0.996	0.986
188	14	0.375	0.291	0.314	0.418	0.482	0.473	0.514	0.602	0.734	0.683	0.082	0.911	0.878	0.727	0.887
188	15	0.366	0.394	0.438	0.463	0.521	0.592	0.704	0.787	0.861	0.944	0.991	1.039	1.127	1.171	1.182
188	16	0.381	0.395	0.431	0.469	0.534	0.616	0.723	0.818	0.904	0.967	1.011	1.148	1.148	1.177	1.219

Figure 15: Frequency Curve for Apete Profile 4

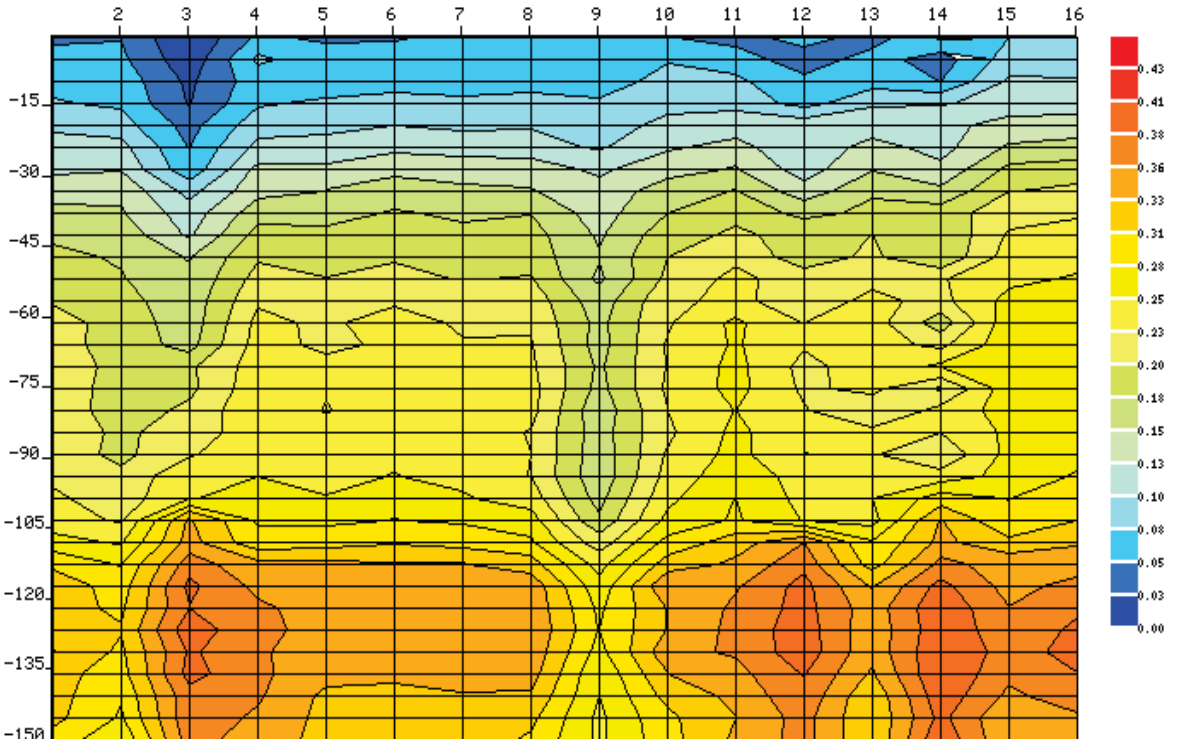
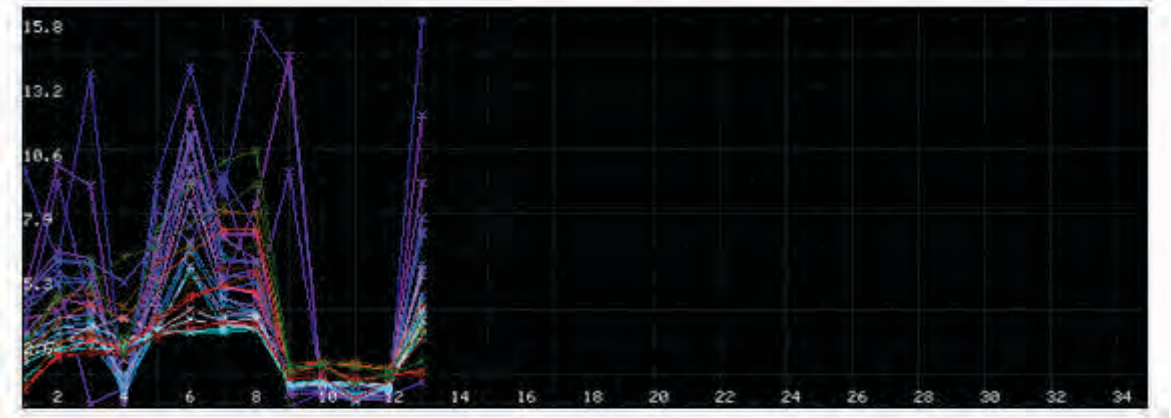


Figure 16: NEF- Profile Map for Apete Traverse 4



1	N	Freq 01	Freq 02	Freq 03	Freq 04	Freq 05	Freq 06	Freq 07	Freq 08	Freq 09	Freq 10	Freq 11	Freq 12	Freq 13	Freq 14	Freq 15
189	1	9.386	4.729	3.124	4.746	3.617	4.298	4.332	4.677	4.712	4.665	3.971	3.003	2.986	2.71	2.796
189	2	6.075	9.976	9.268	5.73	3.935	5.057	5.454	6.023	6.421	6.041	5.109	4.505	3.711	3.676	3.262
189	3	13.735	9.078	3.967	3.935	5.368	0.112	5.126	5.834	6.093	5.983	5.143	4.229	3.797	3.59	3.452
189	4	0.476	0.523	0.564	0.592	0.644	0.747	0.865	0.659	0.017	5.161	0.708	2.295	0.747	1.184	0.535
189	5	9.389	4.263	8.077	8.819	6.817	5.454	5.627	6.559	6.265	6.743	5.109	4.591	4.056	3.676	3.248
189	6	13.983	10.963	6.776	7.456	9.986	11.167	4.219	12.237	12.237	4.098	9.976	9.268	8.405	6.731	6.438
189	7	8.285	5.661	9.268	9.562	7.145	5.35	5.316	6.179	6.955	6.02	4.781	4.902	4.473	4.522	4.177
189	8	25.758	8.336	4.418	7.335	7.145	5.661	5.437	5.937	6.075	6.02	5.161	4.66	4.142	3.849	3.849
189	9	23.756	14.446	9.717	0.025	0.543	0.495	0.701	0.782	0.891	0.887	0.851	0.815	0.806	0.963	0.887
189	10	0.426	0.501	0.535	0.576	0.592	0.651	0.735	0.842	0.889	0.956	0.872	0.889	0.965	1.022	1.023
189	11	0.305	0.287	0.383	0.219	0.596	0.264	0.63	0.618	0.373	0.884	0.832	0.875	0.915	0.983	0.946
189	12	0.438	0.293	0.464	0.493	0.525	0.587	0.658	0.713	0.82	0.799	0.801	0.813	8.761	0.882	0.922
189	13	25.861	12.012	1.063	7.232	7.197	7.18	7.801	7.094	9.23	7.767	5.818	5.644	5.368	4.591	4.332

Figure 17: Frequency Curve for Apete Traverse 5

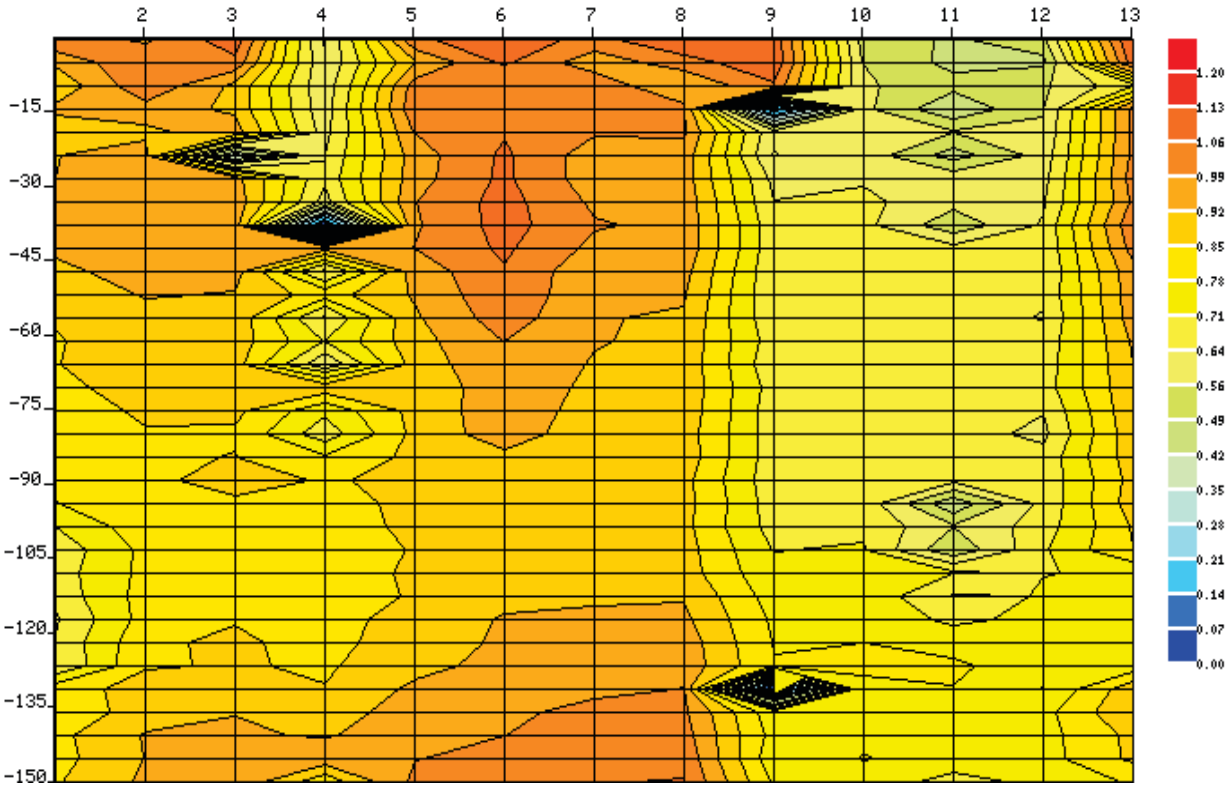


Figure 18: NEF-Profile Map for Apete Traverse 5

routes migrating through fractures and weathered rocks, as observed from the topsoil to the water table. However, Ravn *et al.*, (2020) and Aharoni *et al.*, (2020) affirmed that the areas contaminated by leachates expose the users of such water to danger in the long run. The mobility of leachates down to the subsurface within the cassava processing site as observed in NEF results is quite consistent. The observed deviation in NEFT5 served as the control site located 500 m away from the cassava processing site (to the south) with the entire traverse zone showing no evidence of a leachate plume while due to the weathered and fractured nature of basement complex rocks which must have possibly enhance infiltration, the observed relative distribution of high conductivity values is a revelation of leachates contamination occurrence in the area, with unprecedented impacts on the groundwater quality system. Based on this revelation, the relevance of magnetotelluric technique of geophysical investigation is not to evaluate the subsurface groundwater quality (such as physical and chemical parameters of water) but to assess the extent of subsurface interaction between the aquiferous media and the contaminated zone, since leachate's pathways to aquiferous media are principally governed by gravity (Adagunodo *et al.*, 2023). Gravity freely allows leachates to flow vertically and laterally within the subsurface under the influence of rainfall, until it is able to interact with the nearest aquifer along the flow-path (William *et al.*, 2002; Daniel *et al.,* 2021). Though, Adeniji *et al.*, 2024 delineated low resistivity zone with identified values that ranged from 0.0 to 4.92 mV around Ojoou-Olayanju's Dumpsite, Ada, Southwestern Nigeria and while Alabi *et al.*, 2022 reported low resistivity values

that ranged from 0.0 to 4.35 mV in Kobape area of Ogun State, South-West Nigeria. Still, there seemed to be no single, size-fits-all threshold potential difference value that can be used for the delineation of contaminated subsurface. The specific value would depend on various factors like the type of contaminants, adopted measurement method and regulatory standards for soil contamination.

5.0 CONCLUSION

This study gave insight into the effects of Natural Electric Field utilizing magnetotelluric technique of electromagnetic method in the Earth's Conductivity Assessment in relation to assessing the leachate impact and extent on the groundwater quality in Apete; a typical cassava processing site in South-West Nigeria. The natural electric field (NEF) technique gave a deeper understanding of subsurface contamination from invading leachate infiltration in the study area by delineating the contaminant zone from the uncontaminated zone and its capacity of proffering continuous subsurface information for a profile in a typical cassava processing site, subsurface components identification, as well as the evaluation of topsoil characteristic response and variation to change in potential difference in relation to subsurface layers beneath them. The contaminant's vertical infiltration from surface down to the groundwater unit at the subsurface was discovered through analysis and processing of the acquired data. The results were displayed in blue colour codes across the geo-NEF outputs, in which the subsurface structure depicts the topsoil, the fractured/weathered layers, rock contact and fresh basement and the porous and permeable subsurface which revealed the aquiferous zones in the study area. According to the geophysical analysis, the extremely soft terrain, also known as the fractured zone, permitted easy flow cassava effluents emanating from the surface swiftly reaching the subsurface with unprecedented impacts on the groundwater system of the study area. In the entire investigated area, zone 1 in NEFT is predominantly invaded by leachates to a depth of about 30 m to 35 m; zone 2 with potential difference values ranging from 0.40 mV to 0.52 mV, partially affected by the leachate plume; and zones 3 and 4 did not show any significant impact from the leachate plume. The result of NEFT2 trending northward to southward orientation with revealed concentrated plumes at depths ranging from 0 to 15 m, 0 to 38 m, 0 to 28 m, and 5 to 45 m, respectively with most identifiable zones for borehole developments associated with high yields due to the very high pattern of the conductive media. NEFT3 was trending from West to East orientation; the map categorized the area into three principal distinct layers. The first layer indicates the presence of leachates, which extends across the entire map from the left flank to the right flank. The leachate's depths varied from about 15 m (at the West) to a depth < 30 m at the East. The second layer revealed a contrast in conductivity, though with no evident leachate plume is evident in this layer and the final layer revealed the signature of a fresh basement. In NEFT 4, the result of NEF measurement trending from east to west direction revealed the average extent of downward flow of leachates to about 30 m from the surface. It is therefore advisable to drill to about 45 m, 40-60 m and 40-90 m at distance 6-10 m, 12-20 m and 22-32 m which correspond to data points 3-5, 6-10

and 11-16, respectively if uncontaminated groundwater is to be exploited while on the control site, in NEFT5 that trended from West to East direction, with a total length of 26 m, the entire traverse zone does not show any evidence of a leachate plume concentration. The 2D geo-section of the interpreted profile map indicated that there were no clear potential difference signatures to classify the identified layers as polluted. The NEFT location and direction was at 500 m away from the cassava processing site to the south, which acted as the control profile. The specific value of resistivity would depend on various factors like the type of contaminants, adopted measurement method and regulatory standards for soil contamination. Also, though PQWT is capable of detecting variations in electric potentials, it does not provide specific rage of millivolt values for contaminated soil without more detailed information about the geological context, the type and concentration of contaminants and the sensitivity and calibration of equipment used in detecting variation in potential difference. It is therefore recommended that the groundwater system most especially the shallow hand-dug wells within the study area should be sampled in standard laboratories for contaminant loads.

REFERENCE

Adagunodo, T. A., Ojoawo, A. I., Anie, N. O., and Edukugho, P. O. (2023). Application of Frequency Selection and Geoelectrical Sounding Methods for Mapping of Leachate's Pathways in an Active Dumpsite, *SN Applied Sciences*. vol. 5(1), p.352 – 355.

Adejumo, S.A. (2018). Vertical Electrical Sounding Investigation for Groundwater Development in a Crystalline Basement Complex Terrain; A Case Study of Idi-Oro Apete, Southwestern Nigeria. *Global Scientific Journals.* vol. 6(4), p.252. www.globalscientificjournal.com.

Adeniji A. A. Ajani O. O., Adagunodo T. A., and Kolawole T. (2024). Investigation of Leachate Infiltration on Groundwater using Geo- Resistivity and Natural Electric Field Method around Ojoou-Olayanju's Dumpsite, Ada, Southwestern Nigeria. *Nigerian Journal of Technology (NIJOTECH)*. vol. 43(1), p.159 – 171. www.nijotech.com.

Aharoni, I., Siebner, H., Yogev, U., and Dahan, O. (2020). Holistic Approach for Evaluation of Landfill Pollution Potential from the Waste to the Aquifer. *Sci Total Environ*. vol. 741, p.140 – 367.

Ahmed, S. A., and Ali, M. (2004). Partnerships for Solid Waste Management in Developing Countries: Linking Theories to Realities, *Habitat Int*, vol. 28(3), p.467-479.

Akiang, F., Emujakporue, G.O and Nwosu, L.I. (2022). Leachade Delineation and Aquifer Vulnerability Assessment using Geo-Electric Imaging in a Major Dumpsite Around Calabar Flank, Southern Nigeria. *Journal of Environmental Monitoring and Assessment*. vol. 195(1), p.34

Alabi, A. A., Popoola, O. I., Olurin, O. T., Ogungbe, A. S., Ogunkoya, O. A., and Okediji, S. O. (2020). Assessment of Groundwater Potential and Quality using Geophysical and Physicochemical Methods in the Basement Terrain of Southwestern, Nigeria. *Environmental Earth Sciences*. vol. 79 (1), p.364.

Alabi, A. A., Ganiyu, S. A., Idowu, O. A., Ogabi, A. F., Popoola, O. I., and Coker, J. O. (2022). Mapping of Aquifer units in a Complex Geologic Terrain using Natural Electric Field and Electrical Resistivity Techniques. *Ife Journal of Science.* vol. 24(2), p.419-432. https://dx.doi.org/10.4314/ijs.v24i2.19

Amanambu, A. C. (2015). Geogenic contamination: Hydrogeochemical Processes and Relationship in Shallow Aquifers of Ibadan, South-West Nigeria. *Bulletin of Geography. Physical Geography*. Series 9(1), p.5-20. https://doi.org/10p.1515/bgeo-2015-0011

Aweto K.E (2023). Application of Geophysical and Geochemical Approach to Environmental Impact Assessment around Cassava Mills in Western Niger Delta, Nigeria. *Nigerian Journal of Pure and Applied Science*. vol. 36 (1), p.4573-4581

Badmus, G. O., Ogungbemi, O. S., Enuiyine, O. V., Adeyeye, J. A., and Ogunyemi, A. T. (2022). Delineation of Leachate Plume Migration and Appraisal of Heavy Metals in Groundwater around Emirin Dumpsite, Ado-Ekiti, Nigeria. *Scientific African*. vol. 17, p.1308.

Cagniard, L. (1953). Basic Theory of the Magnetotellurics Method of Geophysical Prospecting, *Geophysics*. vol. 18(1), p.605-635.

Carpenter, P. J. and Reddy, K. R. (2011). Refuse Conductivity Variations following Leachate Injection in a Bioreactor Land Fill Cell: Modeling EM Results and Comparison With Well Logs, in *Proceedings of the Symposium on the Application of Geophysics to Engineering and Environmental Problems (SAGEEP*'11). vol. 24(1), p.76.

Clark, L. (1985). Groundwater Abstraction from Basement Complex Areas of Africa. *Quart. J.Eng. Geology.* vol. 18(1), p.25-34.

Daniel, A. N., Ekeleme, I. K., Onuigbo, C. M., Ikpeazu, V. O., and Obiekezie, S. O. (2021). Review on effect of Dumpsite Leachate to the Environmental and Public Health Implication, *GSC Advanced Research and Reviews.* vol. 7(2), p.51-60.

Dare, O. and Fatoba, J. T. (2014). 2D Electrical imaging surveys for leachate plume migration at an old dump site in Ibadan South Western Nigeria: A Case Study.

International Journal of Geophysics. vol. 2014(1), p.879530. http://dx.doi.org/10.1155/2014/879530

Egbinola, C. N. and Amanambu, A. C. 2014. Groundwater Contamination in Ibadan, South-West Nigeria. *SpringerPlus,* vol. 3(1), p.2-7. https://doi.org/10.1186/2193-1801-3-448.

El-Maguiri, A., Kissi, B., Idrissi, L., and Souabi, S. (2016). Landfill Site Selection Using GIS, Remote Sensing and Multicriteria Decision Analysis: Case of the City of Mohammedia, Morocco. *Bull Eng Geol Environ*. vol. 75, p.1301-1309 https://do i.org/10.1007/s10064-016-0889-

Gomo, M. (2023). Use of Electric Potential Difference in Audio Magnetotelluric (AMT Geophysics for Groundwater Exploration. *Groundwater for Sustainable Development*. vol. 20(1), p.100864.

Guru, B., Karthik, S., and Somnath, B. (2017). Frequency Ratio Model for Groundwater Potential Mapping and Its Sustainable Management in Cold Desert, India. *Journal of King Saud University of Science*. vol. 29(3), p.333-347.

Harinath, V. (2020). Introduction PQWT Groundwater detector PQWT-TC Series. p. 11-52.

Heiling, B., Lichtenberger, J., and Beggan, C. (2018). Natural Sources of Geomagnetic Field Variations, *CERN Report No. CERNACC- 2018-0033*; CLIC-Note 108p.

Hunan, P. (2017). Development History and Practical application of Geophysical Prospecting Instrument for Natural Electric field. *Geologic Exploration Equipment Institute, China.*

Hunan, P. (2018). The Principle and Research of Natural Electric Geophysical Prospecting Instrument. *Geologic Exploration Equipment Institute, China.*

Itoba-Tombo E. F., Ntwampe, S. K.O. and Mudumbi J.B.N. (2017). Leaching of Cyanogens and Mycotoxins from Cultivated Cassava into Agricultural Soil: Effects on Groundwater Quality. *INTECHOPEN Publishing Company.* http://dx.doi.org/10.5772/intechopen.68715

Izah S.C, Bassey S.E. and Ohimain E.I. 2017. Change in Treating some Physico-Chemical Properties of Cassava Mill Effluents using Saccharomyces Cerevisiae. *Toxics*. vol. 5(4), p.28.

Keary, P., Brooks, M and Hill, I. 2002. An Introduction to Geophysical Exploration. 3rd Edition. *Blackwell Publishing*. 262p.

Legchenko, A., Baltassat, J., Beauce, A., and Bernard, J. (2002). Nuclear Magnetic Resonance as a Geophysical Tool for Hydrogeologists. *Journal of Applied*

Geophysics. vol. 50(1), p.21-46. ,

Lowrie, W. (2007). Fundamentals of Geophysics (2nd Ed.). *Cambridge University Press*. 393p.

MacDonald, A. M., Bonsor, H. C., Dochartaigh, B. E. O. and Taylor, R. G. 2012. Quantitative Map of Groundwater Resource in Africa. *Environmental Research Letters*, vol. 7, p.1 – 7.

Mor, S., and Ravindra, K. (2016). Leachate Characterization and Assessment of Groundwater Pollution Near Municipal Solid Waste Landfill Site. *Environ Monitor Assess*. vol. 118(1), p.435-456.

Obueh H.O and Odesiri-Eruteyan E. (2016). A Study on the Effects of Cassava Processing Wastes on the Soil Environment of a Local Cassava Mill. *Journal of Pollution Effects and Control*. vol. 4(4), p.4-5. doi:10.4176/2375-4397.1000177

Odjugo, P. A. O. (2009). The Impact of Climate Change on Water Resources: Global and Nigerian Analysis. *FUTY Journal of the Environment*. vol. *4*(1), p.59-774. https://doi.org/10.4314/fje.v4i1.48005.

Okpoli C. C. (2013). Application of 2D electrical resistivity tomography in landfill site: a case study of Iku, Ikare Akoko, Southwestern Nigeria. *Journal of Geological Research*. vol. 2013 (1), p.895160

Olorunfemi, M.O. and Fasuyi, S.A. (1993). Aquifer Types and Geoelectric / Hydrogeological Characteristics of Parts of the Central Basement Terrain of Nigeria (Niger State). *Journal of African Earth Science*. vol. 16 (1), p.309-317,

Osinowo, O. O., Agbaje, M. A., and Ariyo, S. O. (2020). Integrated Geophysical Investigation Techniques for Mapping Cassava Effluent Leachate Contamination Plume, At A Dumpsite in Ilero, Southwestern Nigeria. *Scientific African*. vol. 8(3), p.1-12.

Oyegoke, S. O., Ayeni, O. O., Olowe, K. O., Adebanjo, A. S., and Fayomi, O. O. (2020). Effectiveness of geophysical assessment of boreholes drilled in basement complex terrain at Afe Babalola University, using electromagnetic method. *Nigerian Journal of Technology*, vol. 39(1), p.36-41.

Oyeyemi, K. D., Olofinnade, O. M., Aizebeokhai, A. P., Sanuade, O. A., Oladunjoye, M. A., Ede, A. N., Adagunodo, T. A., and Ayara, W. A. (2020). Geoengineering site Characterization for Foundation Integrity Assessment. *Cogent Engineering,* vol. 7 (1), p. 1-15. https://doi.org/10.1080/23311916.2020.1711684.

Padmaja, G. (1995). Cyanide Detoxification in Cassava for Food and Feed Uses. Critical Reviews in Food Science and Nutrition, vol. 35(4), p.299 – 339.

Ravn, N. R., Michelsen, A., and Reboleira, A. S. P. S. (2020). Decomposition of Organic Matter in Caves. *Front Ecology, vol.* 8(1), p.171

Rensburg, R. V. (2019). AT receiver pseudo science or a method worth investigating. *Geotron System, Potchefstroom, South Africa.*

Satpathy, B.N. and Kanugo, B.N. (1976). Groundwater Exploration in Hard Rock Terrain. *Geophysical Prospecting.* vol. 24(4), p.725-736

Suleman, K. O., Adagunodo, T. A., Ogunmola, O. L., Adeoye, T. O., Sunmonu, L. A., Alagbe, G. A., Agboola, R. O., Usikalu, M. R., Isibor, P. O., Akinwumi, S. A., Olawole, O. C., and Babarimisa, I. O. (2023). Investigation of Subsurface Contaminants Leachate within Ansaru-Islam Secondary School, Ilorin, Nigeria, *IOP Conf. Series: Earth and Environmental Science,* vol. 1197, p.012011. https://doi.org/10.108 8/1755-1315/1197/1/012011.

Sun, J. L. (2002). Application of Natural Audio Fequency Telluric Method n Detecting Groundwater. *Groundwater.* vol. 24(3), p.181-182.

Theophilus, A.A., Ayobami, I.O., Nicholas, O.A and Praise, O.E (2023) Application of Frequency Selection and Geoelectrical Sounding Methods for Mapping of Leachate's Pathway in an Active Dumpsite. *Springer Nature Jounal.* vol 5(1), p.352.

Ugwu, E.I and Agunwamba,J.C. (2021). Detoxification of Cassava Wastewater by Alkali Degradation. *International Research Journal*. vol. 1(7), p.161-171.

Waff, H. (2000). Electrical Resistivity Imaging of Groundwater Systems using Natural and controlled Source Magnetotellurics, *University of Oregon, Oregon*. 20 p.

WHO (2000). World Health Organization. Global Water Supply and Sanitation Assessment. 22p.

William, M.A., Richard, W.H., James, W.L., and Thomas, E.R. (2002). Flow and Storage in Groundwater Systems. *Science Journal*. vol. 296(5575), p.1985-1990.

Wright, E.P. (1992). The Hydrogeology of Crystalline Basement Aquifers in Africa. *Geological Society, London, special Publications*. vol. 66(1), p.1-27.

Zonge, K. L., and Hughes, L. J. (1991). Electromagnetic Methods in Applied Geophysics: Application, Parts A and B. *Society of Exploration Geophysicists.* vol. 2(1), p.713-810.